Neuroprotection and progenitor cell renewal in the injured adult murine retina requires healing monocyte-derived macrophages

Anat London,[1] Elena Itskovich,[1] Inbal Benhar,[1] Vyacheslav Kalchenko[2], Matthias Mack,[3] Steffen Jung,[2] and Michal Schwartz[1]

[1]Department of Neurobiology and [2]Department of Immunology, Weizmann Institute of Science, Rehovot 76100, Israel
[3]Department of Internal Medicine, University of Regensburg, 93053 Regensburg, Germany

The death of retinal ganglion cells (RGCs) is a hallmark of many retinal neuropathies. Neuroprotection, axonal regeneration, and cell renewal are vital for the integrity of the visual system after insult but are scarce in the adult mammalian retina. We hypothesized that monocyte-derived macrophages, known to promote healing in peripheral tissues, are required after an insult to the visual system, where their role has been largely overlooked. We found that after glutamate eye intoxication, monocyte-derived macrophages infiltrated the damaged retina of mice. Inhibition of this infiltration resulted in reduced survival of RGCs and diminished numbers of proliferating retinal progenitor cells (RPCs) in the ciliary body. Enhancement of the circulating monocyte pool led to increased RGC survival and RPC renewal. The infiltrating monocyte-derived macrophages skewed the milieu of the injured retina toward an anti-inflammatory and neuroprotective one and down-regulated accumulation of other immune cells, thereby resolving local inflammation. The beneficial effect on RGC survival depended on expression of interleukin 10 and major histocompatibility complex class II molecules by monocyte-derived macrophages. Thus, we attribute to infiltrating monocyte-derived macrophages a novel role in neuroprotection and progenitor cell renewal in the injured retina, with far-reaching potential implications to retinal neuropathies and other neurodegenerative disorders.

CORRESPONDENCE
Michal Schwartz:
michal.schwartz@weizmann.ac.il

Abbreviations used: CB, ciliary body; CNS, central nervous system; CNTF, ciliary neurotrophic factor; *egfr*, *epidermal growth factor receptor*; GCL, ganglion cell layer; IOP, intraocular pressure; IPL, inner plexiform layer; RGC, retinal ganglion cell; RPC, retinal progenitor cell.

The integrity of the visual system is highly dependent on functional retinal ganglion cells (RGCs). Neuronal death after initial retinal insult leads to a vicious cycle of neurotoxicity that results in spread of damage. The evoked mechanisms of protection and repair are apparently insufficient, resulting in further death of RGCs. The death of these cells is common to many retinal neuropathies and is a major cause of blindness worldwide.

Cell renewal, a common healing process in peripheral tissues, is limited in the adult neural retina (Moshiri et al., 2004; Reh and Fischer, 2006). However, a quiescent population of retinal progenitor cells (RPCs) continues to exist in the retinal ciliary body (CB) throughout adulthood and has the potential to differentiate into various cells of the retina (Ahmad et al., 2000; Tropepe et al., 2000) or to possibly serve as a source of immunomodulatory or neurotrophic agents (Martino and Pluchino, 2006; Gamm et al., 2007; Einstein and Ben-Hur, 2008; Stanke and Fischer, 2010). This dormant progenitor cell niche was reported to be stimulated after retinal injury (Nickerson et al., 2007; Wohl et al., 2009), although the underlying mechanisms are yet to be revealed. Unraveling the healing processes that operate in response to injury and finding ways to enhance them could lead to the development of new therapies for promoting neuroprotection and cell renewal, which is among the research goals in this field (Levin, 2003; Weinreb, 2007; Howell et al., 2008).

A. London, E. Itskovich, and I. Benhar contributed equally to this paper.

The Rockefeller University Press $30.00
J. Exp. Med. Vol. 208 No. 1 23-39
www.jem.org/cgi/doi/10.1084/jem.20101202

The Journal of Experimental Medicine

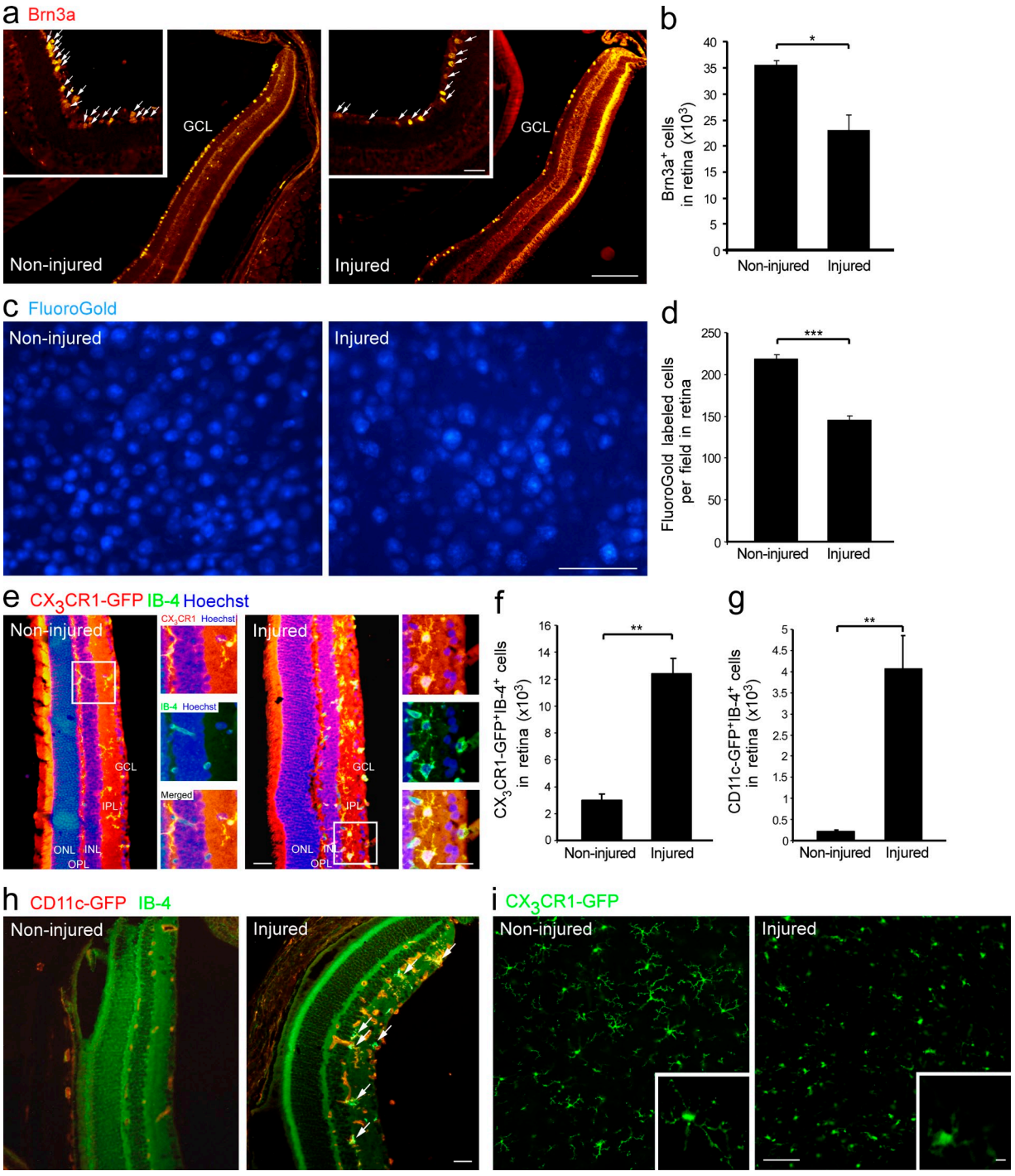

Figure 1. Recruitment and activation of innate immune cells after insult to the inner retina. RGCs were quantified in noninjured and injured retinas 7 d after glutamate intoxication (a–d). (a and b) Brn3a$^+$ RGCs, red (bar, 500 µm). Insets show higher magnification (bar, 100 µm). Arrows indicate Brn3a$^+$ cells. $n = 3$ per group. Data shown are representative of three independent experiments. (c and d) Retrogradely Fluoro-Gold–labeled RGCs, blue (bar, 50 µm). $n = 3$–4 per group. Data shown are representative of five independent experiments. (e and f) Immunohistochemical analysis of noninjured and injured retinal sections from *Cx$_3$cr1*$^{GFP/+}$ mice. CX$_3$CR1, red; myeloid activation marker IB-4, green; Hoechst, blue (bar, 200 µm). Insets show higher magnification of representative CX$_3$CR1-GFP$^+$ myeloid cells (bar, 100 µm). Bar graphs show quantification of CX$_3$CR1-GFP$^+$IB4$^+$ myeloid cells in noninjured and injured retinas. $n = 3$ per group. (g and h) Immunohistochemical analysis of noninjured and injured retinal sections from *CD11c*$^{GFP/+}$ mice. CD11c-GFP, red; IB-4, green (bar, 200 µm). Arrows indicate double-labeled cells. Bar graphs show quantification of CD11c$^+$IB-4$^+$ cells in noninjured and injured retinas. $n = 3$ per group. Data shown are representative of two independent experiments. (i) Confocal imaging of noninjured and injured flat-mount retinas from *Cx$_3$cr1*$^{GFP/+}$ mice (bar, 100 µm). Insets show higher magnification of representative cells (bar, 10 µm). ONL, outer nuclear layer; OPL, outer plexiform layer; INL, inner nuclear layer. Bar graphs throughout figure show mean ± SE of each group. *, $P < 0.05$; **, $P < 0.01$; ***, $P < 0.001$.

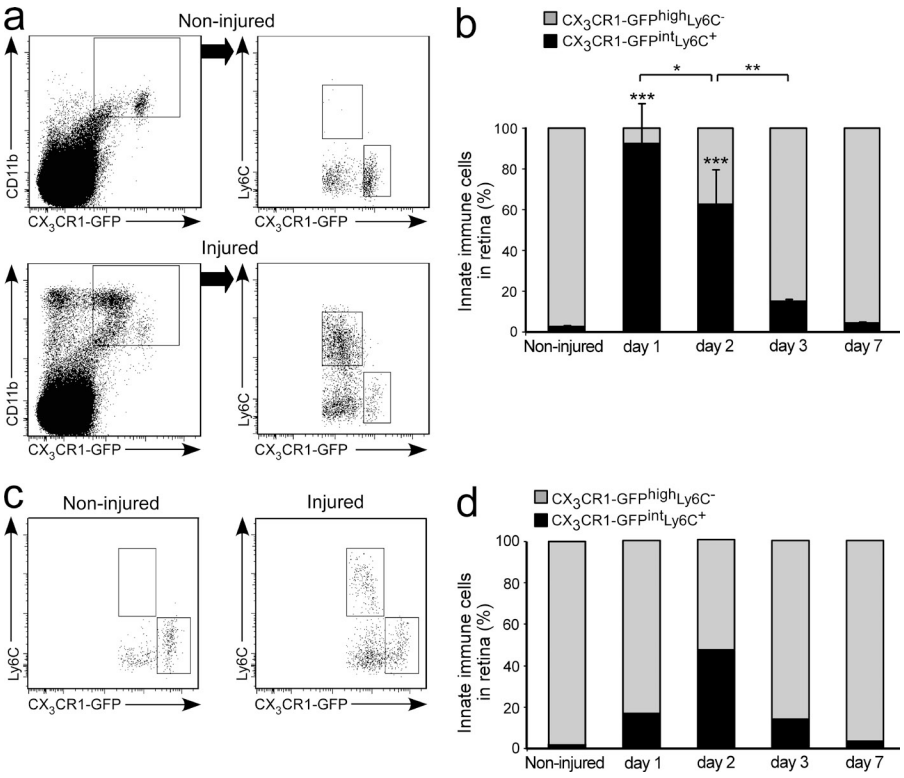

Figure 2. Appearance of a distinct innate immune cell population after insult in models of glutamate intoxication and elevated IOP. Flow cytometric analysis of noninjured and injured retinas from $Cx_3cr1^{GFP/+}$ mice for Ly6C and CX_3CR1-GFP expression on CD11b$^+$ myeloid cells. Cells in dot plots to the right are gated on the CD11b$^+$CX$_3$CR1-GFP$^+$ population (a–d). (a) Note the appearance of the CX$_3$CR1-GFP^{int}Ly6C$^+$ population exclusively in the injured retina. (b) Relative contribution of distinct innate immune populations at different time points after glutamate intoxication. $n = 3$ per group. Bar graphs show mean ± SE of each group. Data shown are representative of two independent experiments. Asterisks above bars indicate significant differences compared with noninjured retina; significant differences between different time points are indicated by asterisks between bars. (c and d) Flow cytometric analysis in the elevated IOP model (pooled data of three animals per group per time point). *, $P < 0.05$; **, $P < 0.01$; ***, $P < 0.001$.

Outside the central nervous system (CNS), healing processes require the help of the immune system for clearance of dead cells and cell debris and for support of regrowth and cell renewal. These processes are mediated, in part, by different subsets of macrophages that acquire discrete phenotypes over the time course of healing. In the course of a response to any insult, there is a pivotal stage of termination of the local immune response involving monocyte-derived macrophages, which contribute to an overall antiinflammatory milieu and produce growth factors needed for regeneration (Gordon and Taylor, 2005; Arnold et al., 2007; Nahrendorf et al., 2007; Weber et al., 2007; Mosser and Edwards, 2008; Geissmann et al., 2010).

The need for neuroprotective agents after injury, together with the beneficial roles of monocyte-derived macrophages in tissue repair in the periphery (Arnold et al., 2007; Nahrendorf et al., 2007; Mosser and Edwards, 2008) and after spinal cord injury (Shechter et al., 2009), has led us to our current hypothesis that infiltrating monocyte-derived macrophages are required for healing of the inner retina after insult.

In the present study, we demonstrated that retinal insult in mice, inflicted in models of glutamate intoxication and elevated intraocular pressure (IOP), evokes vast changes in morphology and activation of innate immune cells. Using BM chimeras, we showed that monocyte-derived macrophages infiltrate the retina only after the insult and localize to the injured ganglion cell layer (GCL). We further discovered that these macrophages support RGC survival and progenitor cell renewal through their ability to skew the retinal milieu toward an antiinflammatory and neurotrophic one. The beneficial effect of these cells on RGC survival was found to be dependent on their expression of the antiinflammatory cytokine IL-10 and of MHC-II molecules.

RESULTS

Characterization of myeloid immune cells after RGC insult

To understand the involvement of myeloid immune cells (resident and infiltrating) in the dynamic events occurring after retinal insult, we first studied this population in the adult retina under physiological and pathological conditions. We chose to use a model of retinal intoxication with glutamate (Schori et al., 2002; Schwartz and Kipnis, 2007), a common mediator of toxicity under neurodegenerative conditions (Dreyer et al., 1996; Shaw and Ince, 1997; Yoles and Schwartz, 1998; Dirnagl et al., 1999; Vorwerk et al., 1999; Gupta and Yücel, 2007). Surviving RGCs were assessed in this study 7 d after glutamate intoxication by immunostaining for Brn3a, a specific RGC marker (Nadal-Nicolás et al., 2009; Fig. 1, a and b), and by retrograde labeling of RGCs with Fluoro-Gold (Fig. 1, c and d), a commonly used method which labels the cell bodies of anatomically intact axons (Schori et al., 2002; Schwartz and Kipnis, 2007). $Cx_3cr1^{GFP/+}$ transgenic mice that carry a GFP reporter under the CX$_3$CR1 promoter (Jung et al., 2000) were used to detect CX$_3$CR1$^+$ cells of the mononuclear myeloid lineage, regardless of their origin (resident or infiltrating). CX$_3$CR1-GFP$^+$ cells were seen both in the naive and intoxicated retinas (Fig. 1 e). Yet, glutamate intoxication resulted in higher numbers of activated

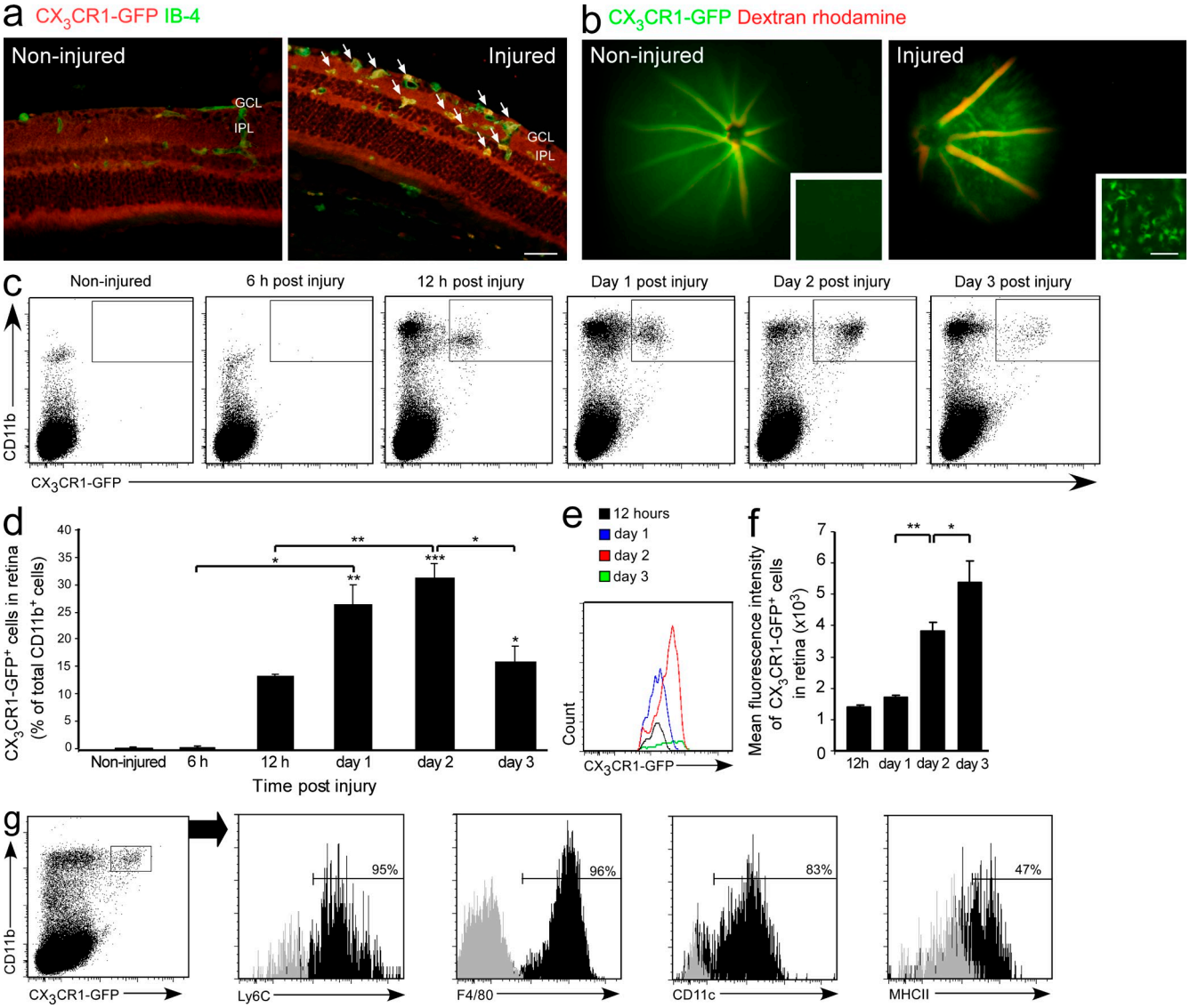

Figure 3. Monocyte-derived macrophages infiltrate the retina after injury. [$Cx_3cr1^{GFP/+}$ > WT] BM chimeric mice were generated and subjected to glutamate intoxication, as described in Materials and methods, and their retinas were analyzed for the presence of infiltrating monocyte-derived macrophages (a–g). (a) Immunohistochemical analysis of retinal sections for activated infiltrating monocyte-derived macrophages. CX_3CR1-GFP, red; IB-4, green (bar, 50 µm). Arrows indicate double-labeled cells. (b) Live imaging of noninjured and injured retinas. Blood vessels were labeled with dextran rhodamine, red. Insets show flat mounts of live-imaged retinas (bar, 50 µm). (c and d) Representative dot plots and their quantitative analysis showing the kinetics of monocyte-derived macrophage infiltration ($CD11b^+CX_3CR1$-GFP^+) after the insult. (e and f) Changes in CX_3CR1-GFP mean fluorescence intensity of the infiltrating monocyte-derived macrophages at different time points after injury. c–f: $n = 3$ per group, per time point. Data shown are representative of two independent experiments. Asterisks above bars indicate significant differences compared with noninjured retina. Significant differences between time points are indicated by asterisks between bars. (g) Expression of distinct markers by the infiltrating monocyte-derived macrophages in the injured retina. Bars demarcate cells positive for the indicated marker (isotype control, gray). Numbers above bars refer to percentage of cells positive for the indicated marker out of the $CD11b^+CX_3CR1$-GFP^+ gated population, representing infiltrating monocyte-derived macrophages. A total of six retinas were pooled and tested for the relevant markers. Data shown are representative of two to three independent experiments. Bar graphs throughout figure show mean ± SE of each group. *, $P < 0.05$; **, $P < 0.01$; ***, $P < 0.001$.

$IB\text{-}4^+CX_3CR1$-GFP^+ myeloid cells, which are mainly located in the proximity of the RGCs (GCL and inner plexiform layer [IPL]; Fig. 1, e and f). Additionally, quantitative analysis showed higher numbers of activated myeloid cells ($IB\text{-}4^+$) expressing CD11c in the intoxicated retina (Fig. 1, g and h) of $CD11c^{GFP/+}$ transgenic mice (Jung et al., 2002). Confocal imaging of whole-mount retinas revealed morphological differences among these innate immune cells under normal versus pathological conditions. In the naive retina, the CX_3CR1-GFP^+ cells had a ramified configuration with extensive processes (Fig. 1 i), a morphology reminiscent of resident/resting microglia (Nimmerjahn et al., 2005). In the injured retina, some of the cells had an ameboid-like shape with smaller processes (Fig. 1 i), indicating activation

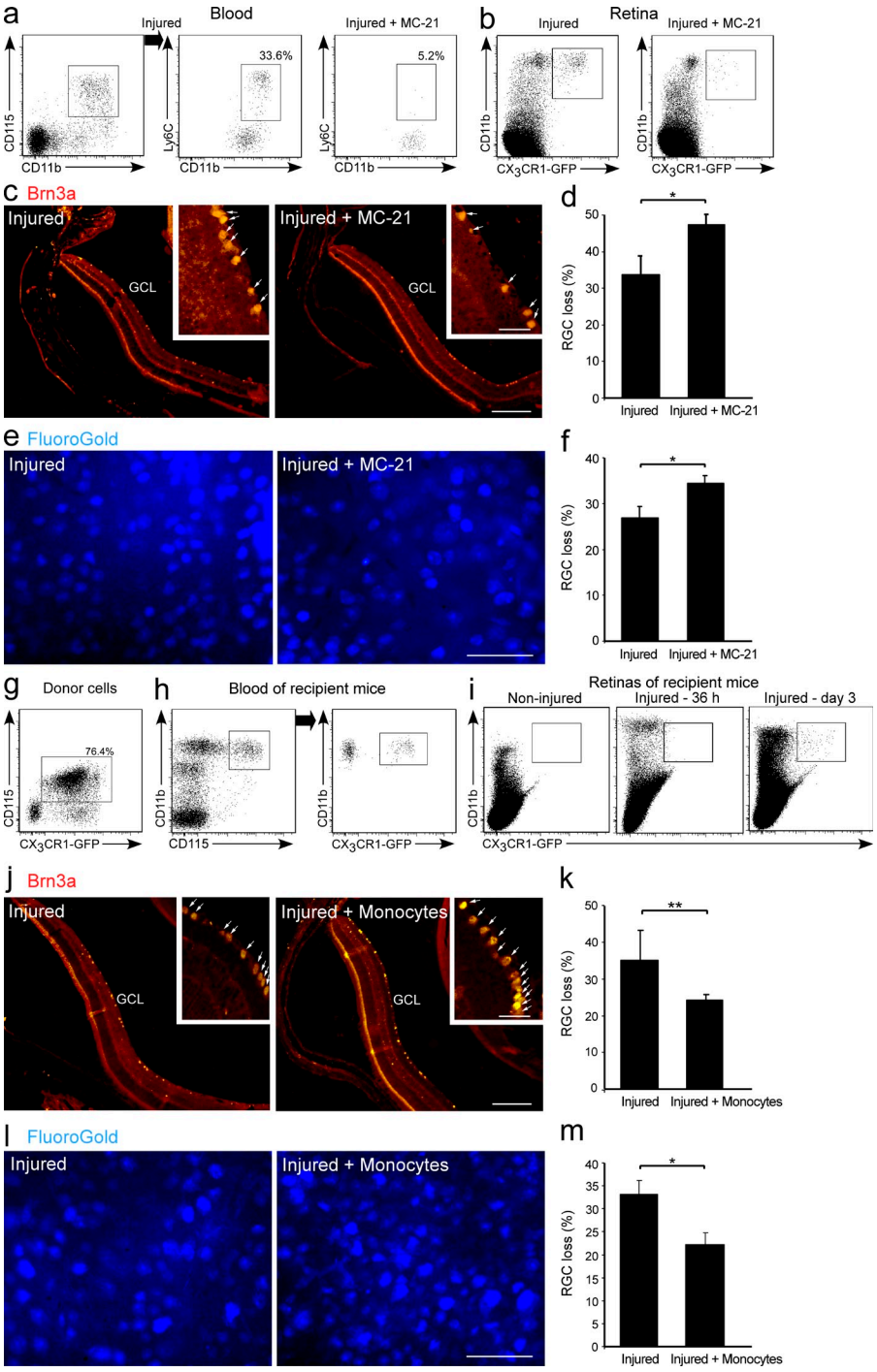

Figure 4. Monocyte-derived macrophages are essential for RGC survival. Glutamate-intoxicated mice were administered the MC-21 antibody and their eyes were analyzed for RGC survival (a–f). (a) Flow cytometric analysis showing the selective depletion of $CD115^+CD11b^+Ly6C^+$ monocytes in the blood. Numbers indicate the percentage of $CD11b^+Ly6C^+$ monocytes out of the total $CD115^+CD11b^+$ monocyte population. $n = 5$ per group. Data shown are representative of six independent experiments. (b) Recruitment of monocyte-derived macrophages ($CD11b^+CX_3CR1\text{-}GFP^+$) to the injured retinas of [$Cx_3cr1^{GFP/+}$ > WT] BM chimeric mice with and without MC-21 treatment. $n = 3$ per group. Data shown are representative of two independent experiments. (c and d) Representative micrographs of retinas stained for the RGC marker Brn3a (red; bar, 500 µm), and respective quantification of RGC loss in MC-21–treated and untreated injured retinas. $n = 5$–8 per group. Data are presented as percentage of RGC loss relative to noninjured retina. Insets show higher magnification of representative $Brn3a^+$ RGCs (bar, 100 µm). Arrows indicate $Brn3a^+$ cells. (e and f) Representative micrographs of RGCs in MC-21–treated and untreated injured retinas stereotactically labeled with Fluoro-Gold (blue; bar, 50 µm) and quantification of RGC loss. $n = 4$–6 per group. Data are presented as percentage of RGC loss relative to noninjured retina. (g–m) Injured mice were adoptively transferred with $CD115^+$ monocytes (WT or $Cx_3Cr1^{GFP/+}$) 1 d after injury, and their eyes were analyzed for RGC survival. Flow cytometric analysis showing the $Cx_3Cr1^{GFP/+}$ donor cells (g) and their presence in the blood of recipient mice (h; cells in dot plot to the right are gated on $CD11b^+CD115^+$ population). (i) Flow cytometric analysis of adoptively transferred cells ($CD11b^+CX_3CR1\text{-}GFP^+$) in noninjured retinas, and in retinas excised 36 h and 3 d after injury. h and i: $n = 3$ per group, per time point. (j and k) Representative micrographs of retinas from injured mice with and without monocyte transfer, stained for the RGC marker Brn3a (red; bar, 500 µm) and respective quantification. $n = 4$ per group, Data are presented as percentage of RGC loss relative to noninjured retina. Insets show higher magnification of representative $Brn3a^+$ RGCs (bar, 100 µm). Arrows indicate $Brn3a^+$ cells. (l and m) Representative micrographs of RGCs in retinas from injured mice with and without monocyte transfer, stereotactically labeled with Fluoro-Gold (blue; bar, 50 µm), and quantification of RGC loss. $n = 4$ per group. Data are presented as percentage of RGC loss relative to noninjured retina. Data shown are representative of two independent experiments. Bar graphs throughout figure show mean ± SE of each group. *, $P < 0.05$; **, $P < 0.01$.

of the existing cells and/or recruitment of an additional myeloid population.

Next, we quantified distinct innate immune populations in naive and injured retinas. Flow cytometric analysis indicated the existence of a $CD11b^+CX_3CR1\text{-}GFP^{high}Ly6C^-$ population in the naive noninjured retina (Fig. 2, a and b). After glutamate intoxication, a discrete population of $CD11b^+CX_3CR1\text{-}GFP^{int}Ly6C^+$ cells was detected (Fig. 2, a and b). To test whether the observed changes in the myeloid immune populations were related to the type of insult or, rather, reflected a general phenomenon evoked by damage to the inner retina, we used another model of retinal insult that also leads to degeneration of

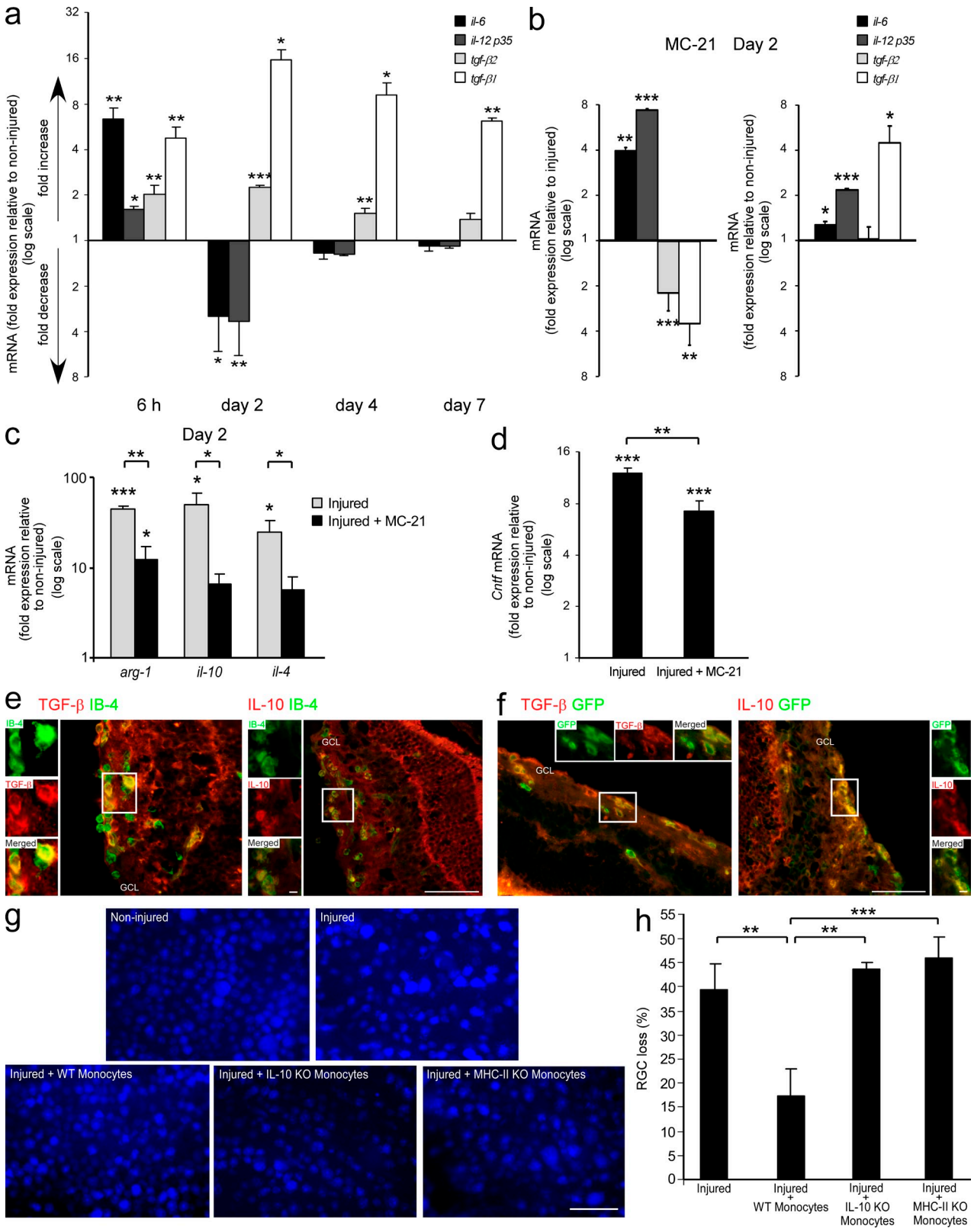

Figure 5. Monocyte-derived macrophages contribute to the neuroprotective and antiinflammatory retinal milieu. (a) Changes in mRNA transcript levels of a series of cytokines in injured compared with noninjured retinas, as a function of time after the insult. (b) Changes in the mRNA transcript levels of various cytokines after MC-21 treatment, compared with injured untreated (left) and noninjured (right) retina. (c) Changes in mRNA levels of additional factors in the injured retina at day 2 after injury, with and without MC-21 treatment, presented relative to noninjured retina. (d) Changes in

RGCs: elevated IOP (Da and Verkman, 2004; Ben Simon et al., 2006). In this model, similar immune changes were observed (Fig. 2, c and d). Collectively, these results demonstrated the appearance of a distinct myeloid cell population after retinal insult and prompted us to consider the possibility that these cells are infiltrating monocyte-derived macrophages.

Infiltrating monocyte-derived macrophages are recruited to the damaged retina

To address the possibility that myeloid cells infiltrate from the blood to the injured retina, we used [*Cx$_3$cr1$^{GFP/+}$* > WT] BM chimeras, whose WT BM had been replaced with that of *Cx$_3$cr1$^{GFP/+}$* mice. In the resulting recipient mice, only infiltrating monocytes were labeled because they derive from donor BM, as opposed to resident microglia which exist in the retina from early ontogeny. This procedure enabled infiltrating monocyte-derived macrophages to be distinguished from resident microglia (Rolls et al., 2008; Shechter et al., 2009). Notably, the heads of the chimeric mice were shielded during the irradiation process, which protected their eyes and brains from any damage other than that induced by glutamate intoxication. In the absence of retinal intoxication, no infiltration of GFP$^+$ cells to the retina could be seen in these chimeras by both immunohistochemical analysis and live in vivo imaging (Fig. 3, a and b), confirming that in the healthy retina there is hardly any turnover of microglia. In glutamate-intoxicated retinas, an infiltration of activated monocyte-derived macrophages was observed at day 2 after injury (Fig. 3, a and b). Importantly, most of the infiltrating cells (77.5 ± 1.9%; mean ± SE) were recruited to the area of lost RGCs, namely the GCL and IPL. Using flow cytometry, we followed the kinetics of infiltration of these cells into the damaged retina. Infiltrating cells were first detected 12 h after injury and peaked at day 2 (Fig. 3, c and d). Notably, at the early stage after injury, the majority of infiltrating cells expressed intermediate levels of the CX_3CR1 receptor, whereas later on most of the cells were CX_3CR1-GFP^{high} (Fig. 3, e and f). In contralateral eyes, which served as control, no infiltrating cells were observed (unpublished data), suggesting the existence of specific recruitment signals in the injured retina. In addition, we evaluated the characteristics and state of activation of the infiltrating CD11b$^+$$CX_3CR1$-GFP$^+$ cells 2 d after injury. Infiltrating cells were found to express Ly6C, F4/80, CD11c, and MHC-II (Fig. 3 g).

Monocyte-derived macrophages promote survival of RGCs after retinal insult

To study the involvement of monocyte-derived macrophages in RGC survival, we used the anti-CCR2 antibody MC-21 (Mack et al., 2001), which selectively depletes CD115$^+$CD11b$^+$Ly6C$^+$ monocytes from the blood (Fig. 4 a). The ablation of circulating Ly6C$^+$ monocytes resulted in decreased recruitment of monocyte-derived macrophages (CD11b$^+$$CX_3CR1$-GFP$^+$) to the injured retina, as assessed in retinas of [*Cx$_3$cr1$^{GFP/+}$* > WT] BM chimeras at day 2 after injury (Fig. 4 b). Ablation of the Ly6C$^+$ monocyte pool resulted in higher RGC loss 7 d after the insult, as indicated by quantitative analysis of Brn3a$^+$ cells in the GCL (Fig. 4, c and d). These results were further confirmed by analysis of retrogradely Fluoro-Gold–labeled cells in whole-mount glutamate-intoxicated retinas (Fig. 4, e and f).

We next tested whether boosting monocyte levels in the blood would lead to enhanced survival of RGCs. To this end, we adoptively transferred 4–5 × 10^6 labeled monocytes (*Cx$_3$cr1$^{GFP/+}$*) into the blood of congenic injured mice, 1 d after injury (Fig. 4, g and h). Flow cytometric analysis indicated that these monocytes could not be detected in the noninjured contralateral retina but were observed in the injured retina at day 3 after the injury (Fig. 4 i). Quantitative analysis of Brn3a$^+$ cells demonstrated higher survival of RGCs 7 d after the injury in mice that were adoptively transferred i.v. with naive monocytes (Fig. 4, j and k). This increased survival was further confirmed by quantifying the number of anatomically intact surviving RGCs using Fluoro-Gold labeling (Fig. 4, l and m). Together, these results demonstrated the neuroprotective role of infiltrating monocyte-derived macrophages in rescuing RGCs after insult. They encouraged us to explore the contribution of monocyte-derived macrophages to the retinal molecular and cellular milieu after injury.

Monocyte-derived macrophages contribute to the neuroprotective and antiinflammatory local milieu of the retina after injury

To evaluate the effect of monocyte-derived macrophages on the local milieu after insult, we analyzed the immunological profile of the retina by quantitative real-time PCR. Within the first 6 h, an elevation in the mRNA transcript levels of the proinflammatory cytokines *il-6* and *il-12-p35*, as compared with

mRNA transcript levels of *cntf* at day 2 after injury, after MC-21 treatment, presented relative to noninjured retina. In a–d, a fold change of 1 indicates no change relative to the relevant control. The numbers situated above 1 indicate a fold increase, whereas the numbers below 1 indicate a fold decrease (values presented on a logarithmic scale). For all experiments, $n = 3$–6 per group, per time point. Data shown are representative of one to two independent experiments. Asterisks above bars represent statistical significance compared with the relevant control. In c and d, asterisks between bars represent statistical significance with respect to the MC-21 treatment. (e) Representative micrographs of retinas from day 2 after injury, showing the expression of TGF-β (red, left) and IL-10 (red, right) by activated IB-4$^+$ myeloid cells (green; bar, 50 µm). Insets show higher magnification of representative double-labeled cells (bar, 5 µm). (f) Representative micrographs of retinas from [*Cx$_3$cr1$^{GFP/+}$* > WT] BM chimeras on day 2 after injury, showing the expression of TGF-β (red, left) and IL-10 (red, right) by infiltrating GFP$^+$ monocyte-derived macrophages (green; bar, 50 µm). Insets show higher magnification of representative double-labeled cells (bar, 5 µm). (g and h) Representative micrographs of Fluoro-Gold–labeled retinas (blue; bar, 50 µm) from noninjured and injured mice without monocyte transfer and from injured mice adoptively transferred with WT, IL-10–deficient, or MHC-II–deficient monocytes. Bar graph shows quantification of RGC loss in the various groups. $n = 4$–6 per group. Data are presented as percentage of RGC loss relative to noninjured retina. Bar graphs throughout figure show mean ± SE of each group. *, $P < 0.05$; **, $P < 0.01$; ***, $P < 0.001$.

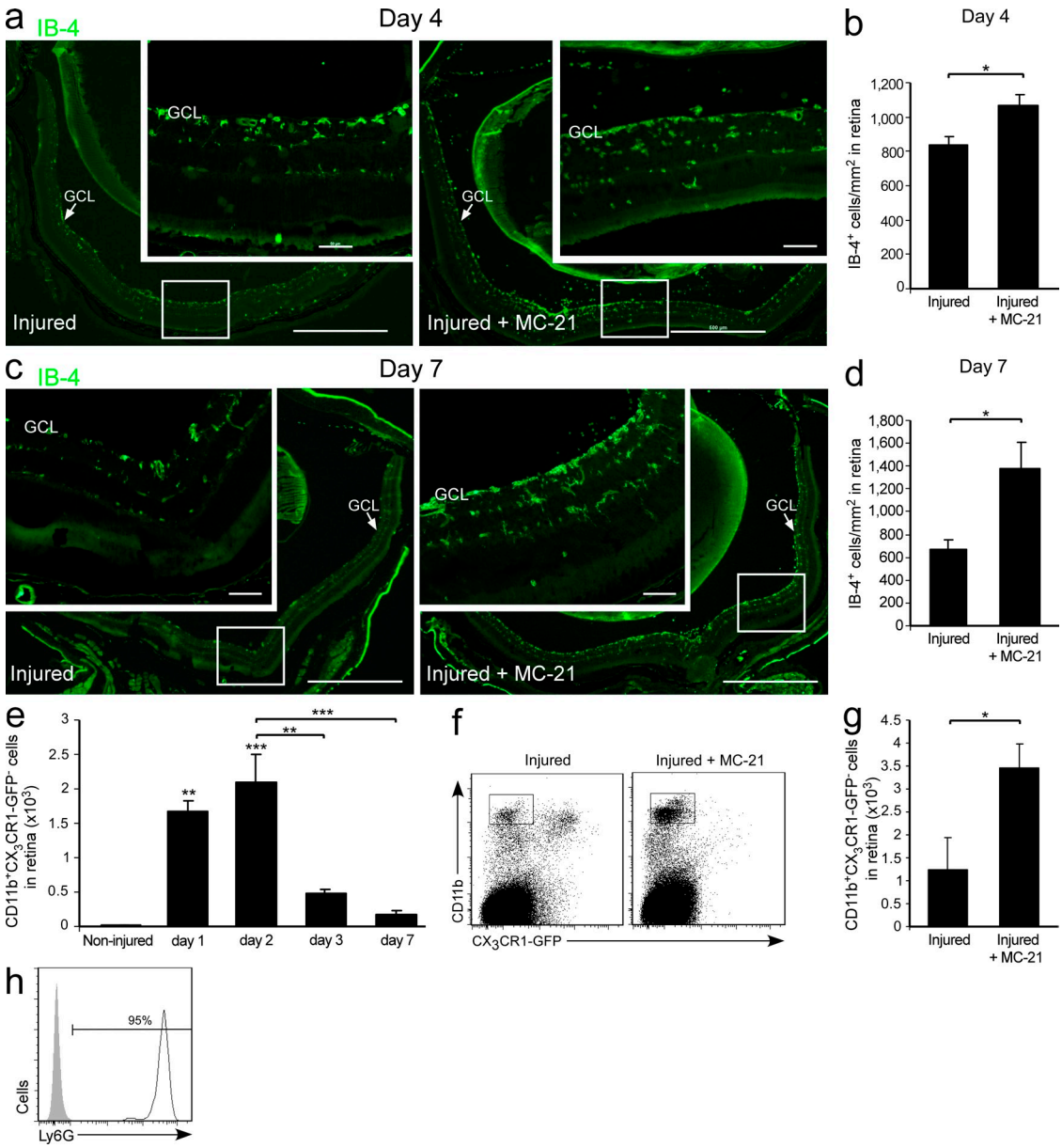

Figure 6. Monocyte-derived macrophages regulate the accumulation of other immune cells in the injured retina. (a–d) Representative micrographs showing activated IB-4+ cells (green; bars, 500 µm) in injured retinas at days 4 and 7 after injury from mice treated with MC-21 compared with untreated injured mice, and respective quantification. $n = 3–5$ per group. Insets show higher magnification (bars, 50 µm). Arrows indicate GCL. (e) Quantitative analysis showing the kinetics of neutrophil ($CD11b^+CX_3CR1\text{-}GFP^-$) accumulation after insult in $Cx_3cr1^{GFP/+}$ transgenic mice. $n = 2–3$ per time point. Asterisks above bars indicate significant differences compared with noninjured retina. Significant differences between time points are indicated by asterisks between bars. (f and g) Flow cytometric analysis and respective quantification, showing the effect of monocyte depletion on neutrophil ($CD11b^+CX_3CR1\text{-}GFP^-$) accumulation after insult. $n = 3–5$ per group. Data shown are representative of two independent experiments. (h) Representative histogram demonstrating the expression of the Ly6G granulocytic marker by $CD11b^+CX_3CR1\text{-}GFP^-$ neutrophils in the injured retina. Bar graphs throughout figure show mean ± SE of each group. *, $P < 0.05$; **, $P < 0.01$; ***, $P < 0.001$.

noninjured retina, was observed (Fig. 5 a). This increase was accompanied by elevated transcript levels of *tgf-β1* and *tgf-β2* (Fig. 5 a), which are commonly considered antiinflammatory cytokines but in the context of IL-6 are able to drive a Th17-mediated proinflammatory response (Bettelli et al., 2006; Mangan et al., 2006; Veldhoen et al., 2006). Thus, at this early time point, before monocyte-derived macrophages could be observed in the retina (Fig. 3, c and d), the overall profile was proinflammatory. We further analyzed IL-6 and TGF-β1 at this time point by ELISA and found a similar trend (85.13 ± 13.90 pg/mg protein vs. 35.78 ± 2.61 for IL-6 and 10.37 ± 3.06 pg/mg protein vs. 4.27 ± 1.30 for TGF-β1, in injured vs. noninjured retinas, respectively; mean ± SE). TGF-β expression was also demonstrated by immunohistochemical staining

on IB-4$^+$ cells (Fig. S1). By day 2 after injury, the time point of peak monocyte-derived macrophage infiltration (Fig. 3, c and d), the immunological profile had shifted toward an antiinflammatory one. This shift was manifested by down-regulation in the mRNA levels of the proinflammatory cytokines *il-6* and *il-12-p35*, along with an up-regulation of the antiinflammatory cytokines *tgf-β1* and *tgf-β2*, as compared with noninjured retinas (Fig. 5 a). A trend toward the resolution of the immunological response was first observed at day 4 after injury and continued through day 7, at which mRNA levels of most of these cytokines, with the exception of *tgf-β1*, were comparable to those in noninjured contralateral retinas (Fig. 5 a). These changes in the immunological milieu of the injured retina, which correlated with the absence or presence of infiltrating monocyte-derived macrophages at 6 h and 2 d after injury, respectively, indicated a possible role of monocyte-derived macrophages in skewing the local milieu toward an antiinflammatory one.

To further establish the role of monocyte-derived macrophages in regulating the immunological milieu, we made use of the MC-21 antibody to deplete the monocyte population in the blood, thereby enabling us to observe the local retinal environment after injury, in the absence of monocyte recruitment. As opposed to the antiinflammatory shift at day 2 after injury (Fig. 5 a), quantitative real-time PCR analysis of retinas from MC-21–treated mice, excised at the same time point, demonstrated a characteristic proinflammatory profile. Namely, mRNA levels of the antiinflammatory cytokines *tgf-β1* and *tgf-β2* were down-regulated, whereas the levels of proinflammatory cytokines were robustly increased, compared with injured mice which had not been treated with MC-21 (Fig. 5 b, left). Importantly, the mRNA levels of *il-6*, *il-12-p35*, and *tgf-β1* in retinas from MC-21–treated mice were elevated compared with noninjured retinas (Fig. 5 b, right), indicating that in the absence of infiltrating monocyte-derived macrophages the proinflammatory environment was not resolved.

To substantiate the contribution of monocyte-derived macrophages to the antiinflammatory milieu, the presence of additional immune components was examined at day 2 after injury. An increase in mRNA levels of the antiinflammatory mediators *il-10*, *il-4*, and *arg-1* was observed. Monocyte depletion prevented the increase in *il-10* and *il-4* transcript levels and attenuated the elevation in *arg-1* (Fig. 5 c), confirming the antiinflammatory influence of these cells. The monocyte-driven effects appear to be specific for certain mediators but not others, as mRNA levels of *tgf-β3*, *il-27*, *il-1β*, and *tnf-α* were not affected by monocyte depletion (not depicted). Adoptive transfer of monocytes further contributed to resolution of the local immune response, as was manifested by a decrease in *tgf-β1* mRNA levels relative to injured retinas from mice that did not receive monocyte transfer (1.5 ± 0.1-fold decrease at day 4, $P < 0.01$, and 2.3 ± 0.3 at day 7 after injury, $P = 0.06$), resulting in levels closer to those of naive noninjured retinas.

The observed effects of monocyte-derived macrophages on neuronal survival prompted us to examine whether these macrophages also affected local expression of neurotrophic factors. We focused on ciliary neurotrophic factor (CNTF), an axogenesis factor for RGCs, which promotes their survival (Jo et al., 1999; Pease et al., 2009). Before monocyte recruitment, namely, at 6 h after injury, mRNA levels of this factor were not changed compared with noninjured retinas (Fig. S2 a). However, at day 2 after the insult, a significant increase was observed, which was attenuated by the depletion of monocytes (Fig. 5 d). These results, together with the findings that adoptive transfer of monocytes did not affect *cntf* levels, as tested at day 7 (Fig. S2 b), suggest that increased *cntf* expression in the injured retina is a monocyte-dependent event that occurs early after their infiltration.

We considered the possibility that the contribution of monocyte-derived macrophages to the restoration of homeostasis is dependent on antiinflammatory cytokines and, therefore, explored the cellular sources of these cytokines. Immunohistochemical analysis of injured retinas from day 2 revealed the expression of TGF-β and IL-10 by activated myeloid cells (IB-4$^+$; Fig. 5 e). By staining sections from [$Cx_3cr1^{GFP/+}$ > WT] BM chimeras, we discovered that these cytokines were expressed by infiltrating monocyte-derived macrophages located at the GCL and IPL (Fig. 5 f). It should be noted that additional cells, other than the monocyte-derived macrophages, appeared to express these cytokines as well.

To examine whether the monocyte-dependent changes in the local milieu are part of the mechanisms by which these cells promote RGC survival, we focused on IL-10, a hallmark of healing antiinflammatory macrophages which is known for its immunosuppressive functions (Moore et al., 2001; Werner and Grose, 2003). To this end, we adoptively transferred injured mice with monocytes from IL-10–deficient donors. Fluoro-Gold labeling indicated that the transferred IL-10–deficient monocytes failed to protect RGCs as compared with WT monocytes, resulting in loss of RGCs similar to that in mice that did not receive monocyte supplementation (Fig. 5, g and h). These results suggest that infiltrating monocyte-derived macrophages contributed to RGC survival by acquiring an antiinflammatory phenotype. In addition, passive transfer of MHC-II–deficient monocytes, similarly to the IL-10–deficient monocytes, failed to contribute to neuronal survival (Fig. 5, g and h).

Monocyte-derived macrophages regulate the accumulation of other immune cells in the injured retina

To further decipher the mechanisms by which monocyte-derived macrophages promote neuroprotection, we turned to investigate how these cells, and the immunoregulatory milieu they promote, affect other immune cells in the retina. Specifically, we tested for immune cells whose unregulated accumulation is known to result in spread of damage after CNS insults, such as activated microglia and neutrophils (Andrews et al., 1999; Liu and Hong, 2003; Gronert, 2010). Retinas were collected at day 4 after injury from mice with and without monocyte depletion by systemic administration of the MC-21 antibody. Depletion of monocytes resulted in

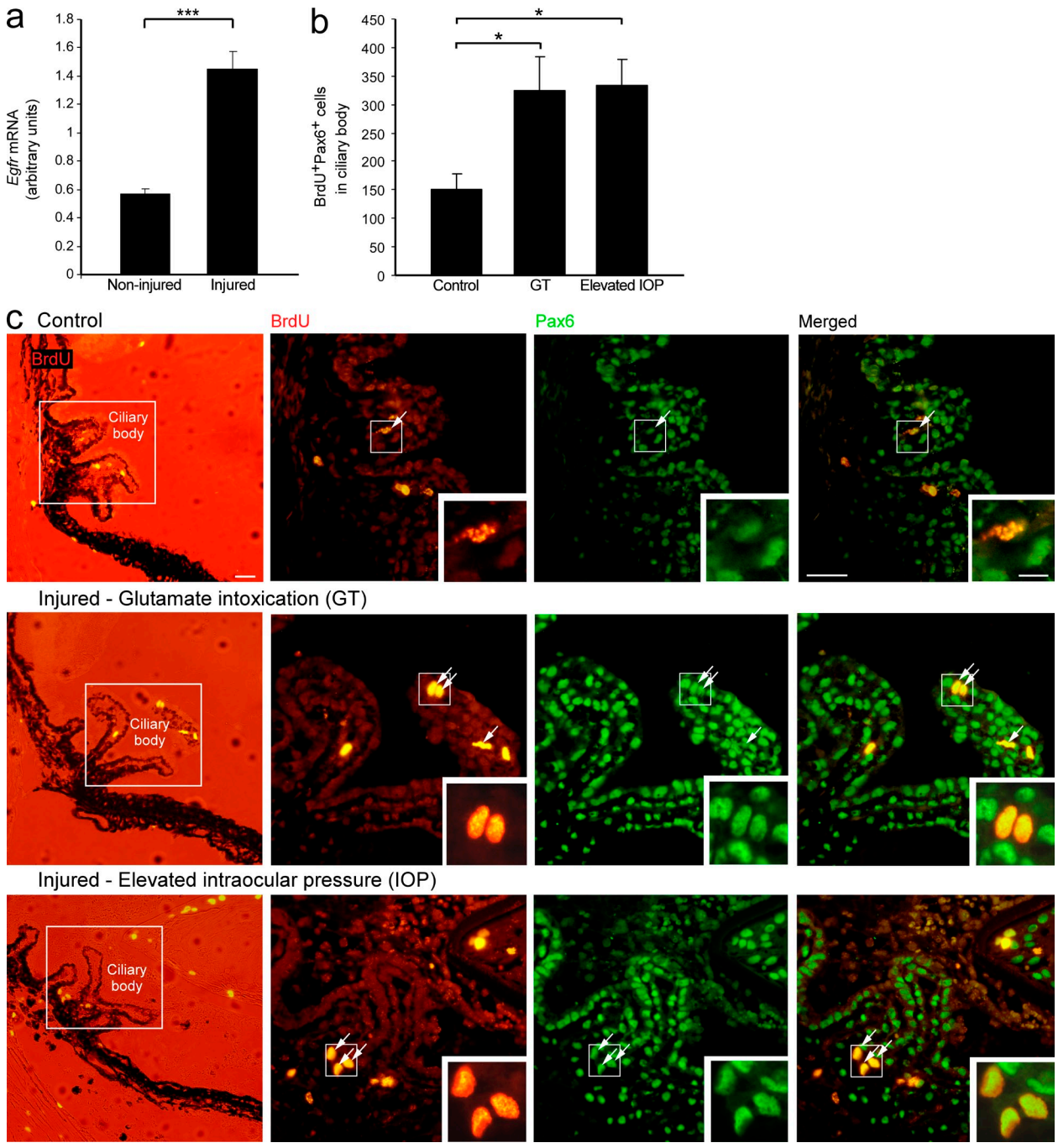

Figure 7. Activation of the quiescent progenitor niche in the adult CB after insult. (a) mRNA levels of *egfr* in noninjured and injured retina. $n = 3–5$ per group. Data shown are representative of two independent experiments. (b and c) Injured and noninjured mice were subjected to a BrdU regimen to label proliferating cells. (b) Quantification of proliferating RPCs ($BrdU^+Pax6^+$) in the glutamate intoxication (GT) and elevated IOP models. $n = 4–6$ per group. Data shown are representative of one (elevated IOP) or two (GT) independent experiments. (c) Representative micrographs of CBs of control (top), glutamate-intoxicated (middle), and elevated IOP (bottom) eyes stained for the cell proliferation marker BrdU (red) and the neural/retinal progenitor marker Pax6 (green; bars, 200 µm in the left column and 100 µm in the other columns). Arrows indicate double-labeled cells. Insets show higher magnification of representative proliferating RPCs (bar, 10 µm). Bar graphs throughout the figure show mean ± SE of each group. * $P < 0.05$, *** $P < 0.001$.

increased accumulation of $IB\text{-}4^+$ cells (Fig. 6, a and b), as compared with injured animals that were not subjected to depletion. At day 7 after injury, results were similar, with a more pronounced effect (Fig. 6, c and d).

With respect to neutrophils, we first used flow cytometry to follow the kinetics of $CD11b^+CX_3CR1^-$ neutrophils to injured retinas of $Cx_3cr1^{GFP/+}$ transgenic mice. These cells were absent from the noninjured retina and peaked at day 2 after

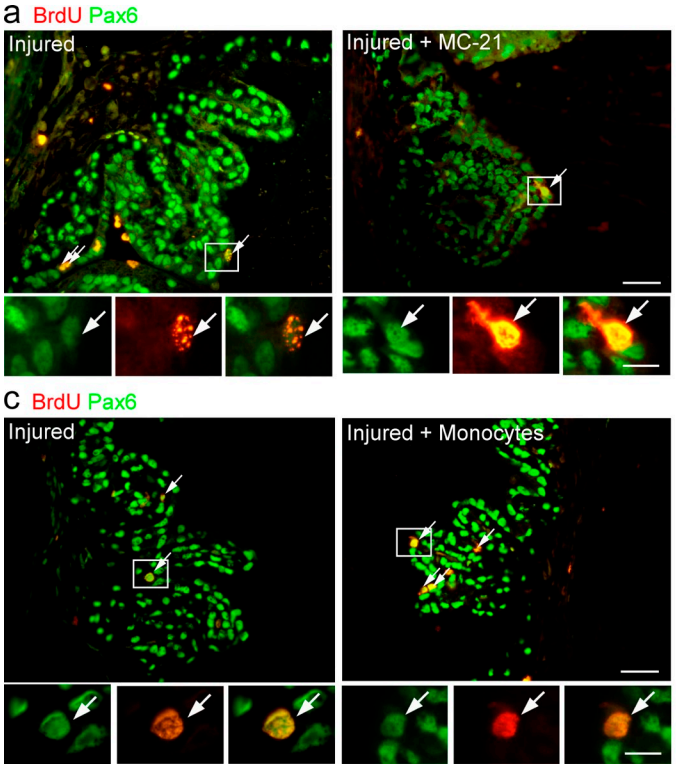

Figure 8. Monocyte-derived macrophages contribute to RPC renewal in the CB of injured adult retina. (a–d) Glutamate-intoxicated mice were either treated with the MC-21 antibody or adoptively transferred with CD115+ monocytes, and their eyes were analyzed for progenitor cell renewal by staining for the cell proliferation marker BrdU (red) and the neural/retinal progenitor marker Pax6 (green). (a and b) Representative micrographs and respective quantification of BrdU+Pax6+ cells in CBs of injured mice with and without MC-21 treatment (bars, 100 µm). $n = 5–6$ per group. Data shown are representative of two independent experiments. (c and d) Representative micrographs and respective quantification of BrdU+Pax6+ cells in CBs of adoptively transferred and untreated injured mice (bar, 100 µm). $n = 3$ per group. Throughout the figure, arrows indicate double-labeled cells; insets show higher magnification of representative proliferating RPCs (bar, 10 µm); and bar graphs show mean ± SE of each group. *, $P < 0.05$.

injury (Fig. 6 e). MC-21–mediated monocyte depletion resulted in elevated numbers of $CD11b^+CX_3CR1^-$ neutrophils at day 2, compared with retinas from injured untreated mice (Fig. 6, f and g). These cells were further characterized by flow cytometry and shown to express the Ly6G marker (Fig. 6 h), which is a common feature of granulocytic neutrophils. Similar results were observed at day 4 after intoxication (not depicted).

Collectively, these results established the immunoregulatory capacity of monocyte-derived macrophages in restricting the accumulation of inflammatory immune cells after acute retinal insult, thereby contributing to restoration of immune homeostasis and to neuroprotection.

Monocyte-derived macrophages support progenitor cell renewal after retinal insult

In light of our findings regarding the contribution of monocyte-derived macrophages to the retinal immunoregulatory and neurotrophic milieu after retinal intoxication, along with the reported involvement of immune cells in regulating CNS progenitor niches (Ziv et al., 2006; Ziv and Schwartz, 2008; Wolf et al., 2009), we next tested whether monocyte-derived macrophages could enhance progenitor cell renewal in the adult retina after injury.

As retinal neurogenesis is generally restricted to the early postnatal stage (Moshiri et al., 2004; Reh and Fischer, 2006), we tested whether the conditions evoked after glutamate intoxication could activate the dormant progenitor niche in the adult CB. Quantitative real-time PCR analysis indicated that glutamate intoxication resulted in higher mRNA levels of *epidermal growth factor receptor* (*egfr*; Fig. 7 a), which is intimately involved in cell renewal and proliferation (Anchan et al., 1991; Close et al., 2006; Giordano et al., 2007), suggesting that the injury did, in fact, induce conditions permissive for cell renewal.

To follow RPC renewal, mice were injected intravitreally with the cell proliferation marker BrdU immediately after injury and for 3 additional consecutive days. Retinal insult resulted in the activation of the dormant progenitor niche; increased numbers of $BrdU^+Pax6^+$ neural progenitor cells could be seen in the CB of intoxicated eyes compared with control eyes 4 d after injury (Fig. 7, b and c). The activation of quiescent progenitors was further verified by the elevated IOP model (Fig. 7, b and c) to control for any direct effect of the glutamate.

To test the contribution of recruited monocyte-derived macrophages to progenitor cell renewal observed after insult, the anti-CCR2 antibody MC-21 was used. In comparison with intoxicated untreated retinas, monocyte ablation resulted in reduced numbers of $BrdU^+Pax6^+$ RPCs in the CB (Fig. 8, a and b), establishing the role of infiltrating monocyte-derived macrophages in supporting cell renewal in the damaged eye. To test whether augmentation of the monocytic pool can enhance progenitor cell renewal beyond spontaneous levels, we performed adoptive transfer of naive monocytes to the injured mice 1 d after injury. This treatment augmented the number of proliferating progenitor cells in the CB (Fig. 8, c and d), further demonstrating the contribution of monocyte-derived macrophages to the activation of the progenitor niche in the adult injured eye. Considering that BrdU was injected for 4 consecutive days, the observed changes in the numbers of proliferating progenitor cells may reflect a monocyte-mediated effect on the survival of these cells rather than an effect on their proliferation alone.

To reveal the fate of the proliferating RPCs observed after insult, we repeated the experiments described in the previous paragraph and collected the eyes 1 wk after the final BrdU injection, a time point suitable for assessing progenitor cell differentiation (Shechter et al., 2008). Immunohistochemical analysis did not show colocalization of $BrdU^+$ cells with any of the neuronal markers tested (unpublished data), namely βIII-tubulin, the bipolar-specific marker PKC-α, and the photoreceptor-specific marker recoverin, suggesting that the RPCs do not engage in cell replacement but can potentially exert neurotrophic or immunoregulatory functions.

DISCUSSION

This study attributes to monocyte-derived macrophages a key role in neuroprotection and progenitor cell renewal after insult to the adult retina, mediated by their antiinflammatory neuroreparative contribution to the local milieu. After glutamate insult, monocyte-derived macrophages infiltrated the damaged retina, almost exclusively to the area of the injured RGCs. Inhibition of this infiltration resulted in excessive loss of RGCs, surpassing the documented clinical threshold which is associated with a detectable vision deficit (Kerrigan-Baumrind et al., 2000; Harwerth and Quigley, 2006). Beyond the positive contribution of endogenous monocyte-derived macrophages, exogenous administration of monocytes resulted in enhanced survival of RGCs. These findings establish the involvement of monocyte-derived macrophages in supporting survival of CNS neurons, the RGCs.

Monocyte-derived macrophages were found to be crucial for the retinal antiinflammatory shift that occurred 2 d after injury. Ablation of the endogenous monocyte pool resulted in reduction of transcripts encoding for the antiinflammatory mediators *tgf-β1/2*, *il-10*, *il-4*, and *arg-1* and an increase in proinflammatory ones. In addition to their role in changing this milieu, the monocyte-derived macrophages regulated the accumulation of activated innate immune cells, thereby promoting restoration of immune homeostasis. These properties suggest that the infiltrating monocyte-derived cells could be regarded as inflammation-resolving macrophages (Bystrom et al., 2008).

Importantly, the neuroprotective effect of monocyte-derived macrophages on RGC survival, which was identified in this study, was found to be dependent, at least in part, upon their potential to produce IL-10. This dependence is consistent with previous studies showing that antiinflammatory cytokines are supportive of neuroprotection (Boyd et al., 2003; Koeberle et al., 2004). This is further corroborated by studies showing that the presence of proinflammatory cytokines has a negative effect on RGC survival. For instance, IL-6 deficiency has been shown to increase survival of RGCs after mechanical and biochemical insults, whereas the reversal of this neuroprotective effect could be achieved by a single IL-6 injection (Fisher et al., 2001b). Notably, we found that adoptive transfer of MHC-II–deficient monocytes also failed to contribute to RGC survival. Thus, the phenotype of cells that mediate neuroprotection is reminiscent of mature myeloid-derived immunosuppressive cells (Movahedi et al., 2008), which, in this case, take part in resolution of the inflammatory response. In addition to their local immunoregulatory contribution, monocyte-derived macrophages also affected the levels of neuroprotective factors such as CNTF and Arg-1, which can directly support neuronal survival (Jo et al., 1999; Pease et al., 2009; Ma et al., 2010).

Considering our current findings regarding the antiinflammatory nature of the infiltrating monocyte-derived macrophages in the injured retina, it is possible that these cells are part of the mechanisms that preserve ocular immune privilege. As an immune-privileged site, the eye uses several strategies to ensure a selective immune repertoire that will provide protection with minimal risk to the integrity of vision (Streilein, 2003). One such mechanism is anterior chamber–associated immune deviation, a form of peripheral tolerance which depends on the infiltration of circulating monocytes to the eye, with these cells eventually reaching the thymus and spleen. There, they induce regulatory T cells that can inhibit cell-mediated immune responses (Streilein, 2003). Interestingly, however, ocular immune privilege may serve as a double-edged sword, as it may result in insufficient monocyte recruitment to the retina under pathological conditions. This notion is strengthened by our finding that increasing the monocyte pool promoted survival of RGCs beyond spontaneous levels. T cell–based vaccination was previously shown to enhance recruitment of monocytes to the injured spinal cord, thereby contributing to functional motor recovery (Shechter et al., 2009). It is thus likely that the neuroprotective effect of T cell–based vaccination, which was previously demonstrated in the injured retina (Fisher et al., 2001a; Schori et al., 2001; Schwartz, 2004; Bakalash et al., 2005; Cortes et al., 2008; Cui et al., 2009), is, in part, a result of enhanced recruitment of monocytes. This issue deserves further investigation.

The use of steroids has been suggested for therapy of various neuropathies. However, studies in the retina have shown the failure of steroids to improve visual outcome after traumatic optic neuropathy in humans (Levin et al., 1999) or to rescue RGCs in various animal models (Solberg et al., 1999; Bakalash et al., 2003; Ohlsson et al., 2004; Dimitriu et al., 2008). In addition, several studies have indicated that immune components provide neuroprotective factors, support axonal regeneration after retinal injury, and mediate IOP reduction (Moalem et al., 1999; Schori et al., 2001; Barouch and Schwartz, 2002; Bakalash et al., 2003, 2005; Yin et al., 2006; Cui et al., 2009; Alvarado et al., 2010). Those studies, together with our identification of a specific macrophage population in the injured retina that is both immunoregulatory and neuroprotective, suggest that overall suppression of the immune system is not only unsuccessful in protecting RGCs but also eliminates the possibility of any potential immune-based protection.

Over the last decade, there has been hope that retinal neuropathies, which are resistant to current therapies, may be treated by administration of stem cells that will proliferate and differentiate to protect or replace retinal neurons. However,

most of the cell replacement therapies tested have been found effective only for peripheral neurons of the retina, such as photoreceptors (Klassen et al., 2004; MacLaren et al., 2006), rather than for RGCs (Johnson et al., 2009), probably because of the fact that successful replacement of RGCs is much more complex as the new cells must extend axons to the superior colliculi of the brain. Other studies have suggested that these stem cells contribute to neuroprotection via immunomodulatory functions and supply of growth factors, rather than serve as a source for cell replacement (Martino and Pluchino, 2006; Gamm et al., 2007; Einstein and Ben-Hur, 2008; Stanke and Fischer, 2010). Because a quiescent RPC population exists in the adult retina (Ahmad et al., 2000; Tropepe et al., 2000), an alternative approach to exogenous stem cell administration would be to stimulate these cells, thereby boosting the endogenous local stem cell pool. In the current study, we demonstrated the contribution of monocyte-derived macrophages to activation of the endogenous progenitor niche after injury. Interestingly, in our paradigm we could not identify any newly generated cells that ultimately integrated into the retina and expressed neuronal markers. We therefore suggest that these proliferating progenitor cells do not engage in cell replacement but might potentially serve as immunomodulators and/or providers of growth factors.

Several studies have shown that a proinflammatory environment can damage progenitor niches (Vallières et al., 2002; Ekdahl et al., 2003; Monje et al., 2003; Rolls et al., 2007; Pluchino et al., 2008; Balasubramaniam et al., 2009). Conversely, an environment that is antiinflammatory and neurotrophic, shown here to be directed by the monocyte-derived macrophages, is known to be supportive of cell renewal (Molina-Holgado et al., 2001; Battista et al., 2006; Ziv et al., 2006; Kiyota et al., 2010), thus presenting a possible mechanism by which these cells contribute to activation of the progenitor niche.

Our results suggest that coping with retinal injury requires a regulated immune response in which monocyte-derived macrophages are essential and intimate partners. Because the main experimental model of this study was glutamate intoxication, a phenomenon relevant to many CNS neurodegenerative disorders (Dreyer et al., 1996; Shaw and Ince, 1997; Yoles and Schwartz, 1998; Dirnagl et al., 1999; Vorwerk et al., 1999), our findings have far-reaching implications that extend beyond the eye. The outcomes of this study suggest the possible therapeutic potential of these cells as unique endogenous neuroprotective agents in treating retinal neuropathies as well as other CNS pathologies that involve neuronal loss.

MATERIALS AND METHODS

Animals. Adult male (8–10 wk old) C57BL/6J mice and heterozygous mutant *Cx$_3$cr1*$^{GFP/+}$ mice (B6.129P-*Cx3cr1*^{tm1Litt}/J, in which one of the CX_3CR1 chemokine receptor alleles is replaced with a gene encoding GFP; Jung et al., 2000) were used. Additionally, C57BL/6J, heterozygous mutant *Cx$_3$cr1*$^{GFP/+}$ mice, MHC-II null mice (B6.129S-*H2*$^{dlAb1\text{-}Ea}$/J), and IL-10 null mice (B6.129P2-*Il10*^{tm1Cgn}/J; Kühn et al., 1993) were used as donors of monocytes and BM. For CD11c detection, *CD11c*$^{GFP/+}$ transgenic mice (B6.FVB-Tg Itgax-DTR/GFP 57Lan/J; Jung et al., 2002) carrying a transgene encoding a GFP reporter under control of the murine CD11c promoter were used. Animals were supplied by the Animal Breeding Center of The Weizmann Institute of Science. All experiments detailed herein conform to the regulations formulated by the Institutional Animal Care and Use Committee of the Weizmann Institute of Science.

BM chimeras. [*Cx$_3$cr1*$^{GFP/+}$ > WT] BM chimeras were prepared by subjecting WT recipient mice to lethal whole-body irradiation (950 rad) while shielding the head, as previously described (Rolls et al., 2008; Shechter et al., 2009). This shielding prevented a direct insult to the retina and any infiltration of myeloid cells other than that induced by glutamate intoxication. On the subsequent day, mice were reconstituted with 5×10^6 BM cells according to a previously described protocol (Shechter et al., 2009). Chimeric mice were subjected to glutamate intoxication 8–12 wk after BM transplantation.

Glutamate-induced toxicity. Mice were anesthetized, treated with local anesthesia (Localin; Dr. Fischer) applied directly to the eye, and injected intravitreally with a total volume of 1 µl saline containing 400 nmol L-glutamate (Sigma-Aldrich), as previously described (Schori et al., 2002).

Elevated IOP model. Ischemic injury was produced as previously described (Da and Verkman, 2004; Ben Simon et al., 2006). In brief, after anesthesia, IOP was elevated by introducing into the anterior chamber a micropipette, connected to a reservoir of isotonic salt solution (Saline). The reservoir was situated at an appropriate height, inducing pressure of 120 mm Hg for 60 min.

MC-21 administration. MC-21 (an antibody to CCR2; Mack et al., 2001) was injected intraperitoneally starting immediately after the injury and throughout the experimental period.

Adoptive monocyte transfer. $CD115^+$ monocytes were isolated as previously reported (Varol et al., 2007). In brief, BM cells were harvested from the femora and tibiae of mice and enriched for mononuclear cells on a Ficoll density gradient. The $CD115^+$ BM monocyte population was isolated through MACS enrichment using biotinylated anti-CD115 antibodies and streptavidin-coupled magnetic beads (Miltenyi Biotec), according to the manufacturer's protocols. After this procedure, monocytes (WT, *Cx$_3$cr1*$^{GFP/+}$, IL-10 deficient, or MHC-II deficient) were injected i.v. ($4–5 \times 10^6$ cells per mouse) on day 1 after injury.

BrdU regimen. BrdU (Sigma-Aldrich) was dissolved in PBS and injected intravitreally (1 µg/eye), immediately after the insult and for 3 consecutive days, according to a protocol adapted from Zhao et al. (2005). Injections were conducted repeatedly through the same hole without additional tissue penetration. Retinas exhibited morphology comparable to those that had received a single injection. Animals were killed 1 d after the last injection to determine the number of proliferating progenitors or 1 wk after the last injection to detect differentiation. Control animals were administered BrdU intravitreally, using the same regimen, in the absence of glutamate intoxication or elevated IOP. Notably, although we cannot rule out a synergistic effect of the injury followed by repeated BrdU injections on the number of proliferating RPCs, because an identical protocol was applied when comparing retinas/ciliary bodies of animals subjected to the different monocyte manipulations, changes in the numbers of proliferating progenitor cells after these manipulations can most likely be attributed to monocyte-mediated effects.

Fluoro-Gold labeling of RGCs. For detection of anatomically intact neurons, mice were injected with 1 µl 5% Fluoro-Gold (Fluorochrome) solution in saline on day 3 after injury to both superior colliculi at the following coordinates: 2.92 mm posterior to the bregma, 0.5 mm lateral to the midline, and at a depth of 2 mm from the skull. After 72 h, the mice were killed, their eyes were enucleated, and each retina was flattened as whole mount in 4% paraformaldehyde (PFA) in PBS. For more details, see Schori et al. (2002) and Schwartz and Kipnis (2007).

Immunohistochemistry. After perfusion with PBS, eyes were removed, postfixed in 2.5% PFA for 24 h, transferred to 70% ethanol, and then embedded into paraffin, as previously described (Shechter et al., 2007). For cytokine staining, eyes were postfixed in 2.5% PFA for 5 h and passed through a gradient of PFA-sucrose. Eyes were then embedded in Tissue-Tek O.C.T. compound (Sakura) and sectioned by cryostat. The following antibodies were used: rabbit anti-GFP (1:100; MBL), rat anti-BrdU (1:100; AbD Serotec), mouse anti-Brn3a (1:50; Santa Cruz Biotechnology, Inc.), rabbit anti-Pax6 (1:100; Covance), mouse anti–TGF-β1, 2, 3 (1:150; R&D Systems), goat anti–IL-10 (1:20; R&D Systems), rabbit anti-βIIIT (1:500; Covance), rabbit anti–PKC-α (1:200; Santa Cruz Biotechnology, Inc.), and rabbit anti-Recoverin (1:1,000; Millipore). The M.O.M. immunodetection kit (Vector Laboratories) was used to localize mouse primary monoclonal antibodies. For activated myeloid cell labeling, FITC-conjugated Bandeiraea simplicifolia isolectin B4 (IB-4; 1:50; Sigma-Aldrich) was added for 1 h to the secondary antibody solution. Secondary antibodies used included Cy2/Cy3-conjugated donkey anti–mouse, –rat, –rabbit, or –goat antibodies (1:150-1:200, all from Jackson ImmunoResearch Laboratories, Inc.). Cy3-streptavidin was used for TGF-β1, 2, and 3 and IL-10 staining. The slides were exposed to Hoechst stain (1:2,000; Invitrogen) for 1 min. For microscopic analysis, a fluorescence microscope (E800; Nikon) or laser-scanning confocal microscope (Carl Zeiss, Inc.) was used. The fluorescence microscope was equipped with a digital camera (DXM 1200F; Nikon) and with either a 20× NA 0.50 or 40× NA 0.75 objective lens (Plan Fluor; Nikon). The confocal microscope was equipped with LSM 510 laser scanning (three lasers: Ar 488, HeNe 543, and HeNe 633) and with a 40× oil-immersion NA 1.3 Plan Neofluor objective lens. Recordings were made on postfixed tissues at 24°C using acquisition software (NIS-Elements, F3 [Nikon] or LSM [Carl Zeiss, Inc.]). Images were cropped, merged, and optimized using Photoshop 9.0 (Adobe) by making minor adjustments to contrast and were arranged using Canvas X (Deneba Software).

Isolation of the retina and flow cytometric analysis. Mice were anesthetized, perfused intracardially with PBS, and their eyes were prepared for flow cytometric analysis. Retinas were removed by dissection and processed to single-cell suspension as previously described (Kerr et al., 2008). The following fluorochrome-labeled mAbs were purchased from BD, BioLegend, or eBioscience and used according to the manufacturers' protocols: PE conjugated anti–MHC-II (I-A/I-E), CD11b, CD115, and Ly6G antibodies; PerCP-conjugated anti-Ly6C antibody; and APC conjugated anti-CD11c, CD11b, and F4/80 antibodies. Cells were analyzed on a FACS LSRII cytometer (BD) using FACSDiva software (BD). Analysis was performed with FlowJo software (Tree Star, Inc.). In each experiment, relevant negative and positive control groups were used to determine the populations of interest and to exclude the rest.

In vivo fluorescence imaging. Mice were anesthetized and gently immobilized using a plastic apparatus. For visualization of the retina, a drop of 0.5% Tropicamide (Dr. Fischer) was used to dilate the pupil and a drop of ophthalmic lubricant (Celluspan; Dr. Fischer) was used to allow placement of a glass coverslip on the eye. Mice were injected with Dextran Rhodamine (1 mg per animal; Sigma-Aldrich) i.v. for blood vessel visualization. Mice were placed under a Zoom Stereo Microscope SZX-RFL-2 (Olympus) equipped with a fluorescence illuminator and a Pixelfly QE charge-coupled device camera (PCO). The excitation and emission for the red filter set were 510–550 nm and 590 nm (long pass), respectively. The green filter set was 460–490 nm for excitation and 510–550 nm for emission. Fluorescence exposure time was 50 ms. Images were acquired using the Camware camera-controlling software program (PCO). Image analysis was performed using ImageJ 1.43 software (W. Rasband, National Institutes of Health, Bethesda, MD).

Quantitative real-time PCR. Mice were anesthetized, perfused intracardially with PBS, and their eyes were prepared for RNA extraction. Retinas were removed by dissection and total RNA was extracted using the RNA MicroPrep kit (Zymo Research). Concentrations and purity of samples were measured by a spectrophotometer (ND-1000; NanoDrop). Random hexamers (Applied Biosystems) were used for first-strand cDNA synthesis. Both procedures were performed according to the manufacturer's instructions. The expression of specific mRNAs was assayed using fluorescence-based quantitative real-time PCR with the following selected gene-specific primer pairs, designed using the Primer Express 3.0 software (Applied Biosystems): *tgf-β1* forward, 5′-TACCATGCCAACTTCTGTCTGGGA-3′ and reverse, 5′-TGTGTTGGTTGTAGAGGGCAAGGA-3′; *tgf-β2* forward, 5′-AATTGCTGCCTTCGCCCTCTTTAC-3′ and reverse, 5′-TGTACAGGCTGAGGACTTTGGTGT-3′; *tgf-β3* forward, 5′-ATTCGACATGATCCAGGGACTGGC-3′ and reverse, 5′-CTCCACTGAGGACACATTGAAACG-3′; *il-6* forward, 5′-TGCAAGAGACTTCCATCCAGTTG-3′ and reverse, 5′-TAAGCCTCCGACTTGTGAAGTGGT-3′; *il-12-p35* forward, 5′-TCACCCTGTTGATGGTCACG-3′ and reverse, 5′-AAATGAAGCTCTGCATCCTGC-3′; *cntf* forward, 5′-AGAGCAATCACCTCTGACCCTTCA-3′ and reverse, 5′-ATCTCACTCCAGCGATCAGTGCTT-3′; *egfr* forward, 5′-ATGCCTTAGCCATCCTGTCCAACT-3′ and reverse, 5′-GTTGCTGAATCGCACAGCACCAAT-3′; and *gapdh* forward, 5′-AATGTGTCCGTCGTGGATCTGA-3′ and reverse, 5′-GATGCCTGCTTCACCACCTTCT-3′.

Reactions were performed using Power SYBR Green PCR Master Mix (Applied Biosystems). The relative amounts of mRNA were calculated using the standard curve method and normalized to a reference gene found to be best suited for our tissue, *gapdh*. Each sample was run in triplicate. Amplification conditions were: 50°C for 2 min, 95°C for 10 min, followed by 40 cycles of 95°C for 15 s, and 60°C for 1 min. Target amplification was first detected between cycles 24 and 26, on average. Dissociation curves showed one species of amplicon for each primer combination.

mRNA levels of *il-4* (assay ID: Mm00445260_m1), *il-10* (Mm00439614_m1), *arg-1* (Mm00475988_m1), *tnfα* (Mm00443258_m1), *il-27* (Mm00461164_m1), and *il-1β* (Mm00434228_m1) were determined using TaqMan Real-Time PCR, according to manufacturer's instructions (Applied Biosystems). cDNA templates were amplified with TaqMan PreAmp Master Mix (Applied Biosystems). Threshold cycle numbers (*Ct*) were determined with 7500 system SDS software (version 1.4; Applied Biosystems) and analyzed using the $\Delta\Delta Ct$ method, as described by the manufacturer, using *gapdh* (Mm99999915_g1) as the calibrator gene. All quantitative real-time PCR reactions were performed using the 7500 Real-Time PCR System (Applied Biosystems).

ELISA. Retinas were dissected, flash frozen, and homogenized on ice in RIPA buffer containing a proteinase inhibitor cocktail (both from Sigma-Aldrich). The samples were centrifuged for 10 min at 8,000 *g* at 4°C. TGF-β1 and IL-6 were assayed in the supernatants using Quantikine kits (R&D Systems), according to the manufacturer's instructions. Cytokine levels were normalized to milligrams of protein, as quantified using the Pierce BCA Protein Assay kit (Thermo Fisher Scientific). The TGF-β1 average for each group represents three independent experiments, containing pooled samples, each comprised of two to six retinas. Single retinas were used for IL-6 ELISA ($n = 4$ in each group).

Statistical analysis. Data were analyzed using a Student's *t* test to compare between two groups. One-way ANOVA was used to compare several groups. Fisher's LSD procedure was used for follow up pairwise comparison of groups after the null hypothesis had been rejected ($F < 0.05$). Results are presented as mean ± SE. In the graphs, y-axis error bars represent SE.

Online supplemental material. Fig. S1 shows the expression of TGF-β by IB-4$^+$ cells 6 h after glutamate intoxication. Fig. S2 depicts *cntf* mRNA expression at 6 h and 7 d after injury. Online supplemental material is available at http://www.jem.org/cgi/content/full/jem.20101202/DC1.

We thank Dr. Tamara Berkutzki for histological processing, Dr. Guy Ben Simon for help with the elevated IOP model, Gilad Kunis for assistance with i.v. injections, Margalit Azoulay for handling the animals, Prof. Edna Schechtman for assistance with analysis of ELISA data, Dr. Hillary Voet for consulation and data presentation, and Shelley Schwarzbaum for editing the manuscript. M. Schwartz holds the Maurice and Ilse Katz Professorial Chair in Neuroimmunology.

The work was supported in part by the Glaucoma Research Foundation.

The authors have no conflicting financial interests.

Submitted: 16 June 2010
Accepted: 14 December 2010

REFERENCES

Ahmad, I., L. Tang, and H. Pham. 2000. Identification of neural progenitors in the adult mammalian eye. *Biochem. Biophys. Res. Commun.* 270:517–521. doi:10.1006/bbrc.2000.2473

Alvarado, J.A., L.J. Katz, S. Trivedi, and A.S. Shifera. 2010. Monocyte modulation of aqueous outflow and recruitment to the trabecular meshwork following selective laser trabeculoplasty. *Arch. Ophthalmol.* 128:731–737. doi:10.1001/archophthalmol.2010.85

Anchan, R.M., T.A. Reh, J. Angello, A. Balliet, and M. Walker. 1991. EGF and TGF-alpha stimulate retinal neuroepithelial cell proliferation in vitro. *Neuron.* 6:923–936. doi:10.1016/0896-6273(91)90233-P

Andrews, D.M., V.B. Matthews, L.M. Sammels, A.C. Carrello, and P.C. McMinn. 1999. The severity of murray valley encephalitis in mice is linked to neutrophil infiltration and inducible nitric oxide synthase activity in the central nervous system. *J. Virol.* 73:8781–8790.

Arnold, L., A. Henry, F. Poron, Y. Baba-Amer, N. van Rooijen, A. Plonquet, R.K. Gherardi, and B. Chazaud. 2007. Inflammatory monocytes recruited after skeletal muscle injury switch into antiinflammatory macrophages to support myogenesis. *J. Exp. Med.* 204:1057–1069. doi:10.1084/jem.20070075

Bakalash, S., A. Kessler, T. Mizrahi, R. Nussenblatt, and M. Schwartz. 2003. Antigenic specificity of immunoprotective therapeutic vaccination for glaucoma. *Invest. Ophthalmol. Vis. Sci.* 44:3374–3381. doi:10.1167/iovs.03-0080

Bakalash, S., G.B. Shlomo, E. Aloni, I. Shaked, L. Wheeler, R. Ofri, and M. Schwartz. 2005. T-cell-based vaccination for morphological and functional neuroprotection in a rat model of chronically elevated intraocular pressure. *J. Mol. Med.* 83:904–916. doi:10.1007/s00109-005-0689-6

Balasubramaniam, B., D.A. Carter, E.J. Mayer, and A.D. Dick. 2009. Microglia derived IL-6 suppresses neurosphere generation from adult human retinal cell suspensions. *Exp. Eye Res.* 89:757–766. doi:10.1016/j.exer.2009.06.019

Barouch, R., and M. Schwartz. 2002. Autoreactive T cells induce neurotrophin production by immune and neural cells in injured rat optic nerve: implications for protective autoimmunity. *FASEB J.* 16:1304–1306.

Battista, D., C.C. Ferrari, F.H. Gage, and F.J. Pitossi. 2006. Neurogenic niche modulation by activated microglia: transforming growth factor beta increases neurogenesis in the adult dentate gyrus. *Eur. J. Neurosci.* 23:83–93. doi:10.1111/j.1460-9568.2005.04539.x

Ben Simon, G.J., S. Bakalash, E. Aloni, and M. Rosner. 2006. A rat model for acute rise in intraocular pressure: immune modulation as a therapeutic strategy. *Am. J. Ophthalmol.* 141:1105–1111. doi:10.1016/j.ajo.2006.01.073

Bettelli, E., Y. Carrier, W. Gao, T. Korn, T.B. Strom, M. Oukka, H.L. Weiner, and V.K. Kuchroo. 2006. Reciprocal developmental pathways for the generation of pathogenic effector TH17 and regulatory T cells. *Nature.* 441:235–238. doi:10.1038/nature04753

Boyd, Z.S., A. Kriatchko, J. Yang, N. Agarwal, M.B. Wax, and R.V. Patil. 2003. Interleukin-10 receptor signaling through STAT-3 regulates the apoptosis of retinal ganglion cells in response to stress. *Invest. Ophthalmol. Vis. Sci.* 44:5206–5211. doi:10.1167/iovs.03-0534

Bystrom, J., I. Evans, J. Newson, M. Stables, I. Toor, N. van Rooijen, M. Crawford, P. Colville-Nash, S. Farrow, and D.W. Gilroy. 2008. Resolution-phase macrophages possess a unique inflammatory phenotype that is controlled by cAMP. *Blood.* 112:4117–4127. doi:10.1182/blood-2007-12-129767

Close, J.L., J. Liu, B. Gumuscu, and T.A. Reh. 2006. Epidermal growth factor receptor expression regulates proliferation in the postnatal rat retina. *Glia.* 54:94–104. doi:10.1002/glia.20361

Cortes, L.M., D. Avichezer, P.B. Silver, D. Luger, M.J. Mattapallil, C.C. Chan, and R.R. Caspi. 2008. Inhibitory peptide analogs derived from a major uveitogenic epitope protect from antiretinal autoimmunity by inducing type 2 and regulatory T cells. *J. Leukoc. Biol.* 84:577–585. doi:10.1189/jlb.0308189

Cui, Q., Y. Yin, and L.I. Benowitz. 2009. The role of macrophages in optic nerve regeneration. *Neuroscience.* 158:1039–1048. doi:10.1016/j.neuroscience.2008.07.036

Da, T., and A.S. Verkman. 2004. Aquaporin-4 gene disruption in mice protects against impaired retinal function and cell death after ischemia. *Invest. Ophthalmol. Vis. Sci.* 45:4477–4483. doi:10.1167/iovs.04-0940

Dimitriu, C., M. Bach, W.A. Lagrèze, and T. Jehle. 2008. Methylprednisolone fails to preserve retinal ganglion cells and visual function after ocular ischemia in rats. *Invest. Ophthalmol. Vis. Sci.* 49:5003–5007. doi:10.1167/iovs.08-1869

Dirnagl, U., C. Iadecola, and M.A. Moskowitz. 1999. Pathobiology of ischaemic stroke: an integrated view. *Trends Neurosci.* 22:391–397. doi:10.1016/S0166-2236(99)01401-0

Dreyer, E.B., D. Zurakowski, R.A. Schumer, S.M. Podos, and S.A. Lipton. 1996. Elevated glutamate levels in the vitreous body of humans and monkeys with glaucoma. *Arch. Ophthalmol.* 114:299–305.

Einstein, O., and T. Ben-Hur. 2008. The changing face of neural stem cell therapy in neurologic diseases. *Arch. Neurol.* 65:452–456. doi:10.1001/archneur.65.4.452

Ekdahl, C.T., J.H. Claasen, S. Bonde, Z. Kokaia, and O. Lindvall. 2003. Inflammation is detrimental for neurogenesis in adult brain. *Proc. Natl. Acad. Sci. USA.* 100:13632–13637. doi:10.1073/pnas.2234031100

Fisher, J., H. Levkovitch-Verbin, H. Schori, E. Yoles, O. Butovsky, J.F. Kaye, A. Ben-Nun, and M. Schwartz. 2001a. Vaccination for neuroprotection in the mouse optic nerve: implications for optic neuropathies. *J. Neurosci.* 21:136–142.

Fisher, J., T. Mizrahi, H. Schori, E. Yoles, H. Levkovitch-Verbin, S. Haggiag, M. Revel, and M. Schwartz. 2001b. Increased post-traumatic survival of neurons in IL-6-knockout mice on a background of EAE susceptibility. *J. Neuroimmunol.* 119:1–9. doi:10.1016/S0165-5728(01)00342-3

Gamm, D.M., S. Wang, B. Lu, S. Girman, T. Holmes, N. Bischoff, R.L. Shearer, Y. Sauvé, E. Capowski, C.N. Svendsen, and R.D. Lund. 2007. Protection of visual functions by human neural progenitors in a rat model of retinal disease. *PLoS One.* 2:e338. doi:10.1371/journal.pone.0000338

Geissmann, F., M.G. Manz, S. Jung, M.H. Sieweke, M. Merad, and K. Ley. 2010. Development of monocytes, macrophages, and dendritic cells. *Science.* 327:656–661.

Giordano, F., A. De Marzo, F. Vetrini, and V. Marigo. 2007. Fibroblast growth factor and epidermal growth factor differently affect differentiation of murine retinal stem cells in vitro. *Mol. Vis.* 13:1842–1850.

Gordon, S., and P.R. Taylor. 2005. Monocyte and macrophage heterogeneity. *Nat. Rev. Immunol.* 5:953–964. doi:10.1038/nri1733

Gronert, K. 2010. Resolution, the grail for healthy ocular inflammation. *Exp. Eye Res.* 91:478–485. doi:10.1016/j.exer.2010.07.004

Gupta, N., and Y.H. Yücel. 2007. Glaucoma as a neurodegenerative disease. *Curr. Opin. Ophthalmol.* 18:110–114.

Harwerth, R.S., and H.A. Quigley. 2006. Visual field defects and retinal ganglion cell losses in patients with glaucoma. *Arch. Ophthalmol.* 124:853–859. doi:10.1001/archopht.124.6.853

Howell, G.R., R.T. Libby, and S.W. John. 2008. Mouse genetic models: an ideal system for understanding glaucomatous neurodegeneration and neuroprotection. *Prog. Brain Res.* 173:303–321. doi:10.1016/S0079-6123(08)01122-9

Jo, S.A., E. Wang, and L.I. Benowitz. 1999. Ciliary neurotrophic factor is an axogenesis factor for retinal ganglion cells. *Neuroscience.* 89:579–591. doi:10.1016/S0306-4522(98)00546-6

Johnson, T.V., N.D. Bull, and K.R. Martin. 2009. Transplantation prospects for the inner retina. *Eye (Lond).* 23:1980–1984.

Jung, S., J. Aliberti, P. Graemmel, M.J. Sunshine, G.W. Kreutzberg, A. Sher, and D.R. Littman. 2000. Analysis of fractalkine receptor CX(3)CR1 function by targeted deletion and green fluorescent protein reporter gene insertion. *Mol. Cell. Biol.* 20:4106–4114. doi:10.1128/MCB.20.11.4106-4114.2000

Jung, S., D. Unutmaz, P. Wong, G. Sano, K. De los Santos, T. Sparwasser, S. Wu, S. Vuthoori, K. Ko, F. Zavala, et al. 2002. In vivo depletion of CD11c+ dendritic cells abrogates priming of CD8+ T cells by exogenous cell-associated antigens. *Immunity.* 17:211–220. doi:10.1016/S1074-7613(02)00365-5

Kerr, E.C., B.J. Raveney, D.A. Copland, A.D. Dick, and L.B. Nicholson. 2008. Analysis of retinal cellular infiltrate in experimental autoimmune

uveoretinitis reveals multiple regulatory cell populations. *J. Autoimmun.* 31:354–361. doi:10.1016/j.jaut.2008.08.006

Kerrigan-Baumrind, L.A., H.A. Quigley, M.E. Pease, D.F. Kerrigan, and R.S. Mitchell. 2000. Number of ganglion cells in glaucoma eyes compared with threshold visual field tests in the same persons. *Invest. Ophthalmol. Vis. Sci.* 41:741–748.

Kiyota, T., S. Okuyama, R.J. Swan, M.T. Jacobsen, H.E. Gendelman, and T. Ikezu. 2010. CNS expression of anti-inflammatory cytokine interleukin-4 attenuates Alzheimer's disease-like pathogenesis in APP+PS1 bigenic mice. *FASEB J.* 24:3093–3102. doi:10.1096/fj.10-155317

Klassen, H.J., T.F. Ng, Y. Kurimoto, I. Kirov, M. Shatos, P. Coffey, and M.J. Young. 2004. Multipotent retinal progenitors express developmental markers, differentiate into retinal neurons, and preserve light-mediated behavior. *Invest. Ophthalmol. Vis. Sci.* 45:4167–4173. doi:10.1167/iovs.04-0511

Koeberle, P.D., J. Gauldie, and A.K. Ball. 2004. Effects of adenoviral-mediated gene transfer of interleukin-10, interleukin-4, and transforming growth factor-beta on the survival of axotomized retinal ganglion cells. *Neuroscience.* 125:903–920. doi:10.1016/S0306-4522(03)00398-1

Kühn, R., J. Löhler, D. Rennick, K. Rajewsky, and W. Müller. 1993. Interleukin-10-deficient mice develop chronic enterocolitis. *Cell.* 75:263–274. doi:10.1016/0092-8674(93)80068-P

Levin, L.A. 2003. Retinal ganglion cells and neuroprotection for glaucoma. *Surv. Ophthalmol.* 48:S21–S24. doi:10.1016/S0039-6257(03)00007-9

Levin, L.A., R.W. Beck, M.P. Joseph, S. Seiff, and R. Kraker. 1999. The treatment of traumatic optic neuropathy: the International Optic Nerve Trauma Study. *Ophthalmology.* 106:1268–1277. doi:10.1016/S0161-6420(99)00707-1

Liu, B., and J.S. Hong. 2003. Role of microglia in inflammation-mediated neurodegenerative diseases: mechanisms and strategies for therapeutic intervention. *J. Pharmacol. Exp. Ther.* 304:1–7. doi:10.1124/jpet.102.035048

Ma, T.C., A. Campana, P.S. Lange, H.H. Lee, K. Banerjee, J.B. Bryson, L. Mahishi, S. Alam, R.J. Giger, S. Barnes, et al. 2010. A large-scale chemical screen for regulators of the arginase 1 promoter identifies the soy isoflavone daidzeinas a clinically approved small molecule that can promote neuronal protection or regeneration via a cAMP-independent pathway. *J. Neurosci.* 30:739–748. doi:10.1523/JNEUROSCI.5266-09.2010

Mack, M., J. Cihak, C. Simonis, B. Luckow, A.E. Proudfoot, J. Plachý, H. Brühl, M. Frink, H.J. Anders, V. Vielhauer, et al. 2001. Expression and characterization of the chemokine receptors CCR2 and CCR5 in mice. *J. Immunol.* 166:4697–4704.

MacLaren, R.E., R.A. Pearson, A. MacNeil, R.H. Douglas, T.E. Salt, M. Akimoto, A. Swaroop, J.C. Sowden, and R.R. Ali. 2006. Retinal repair by transplantation of photoreceptor precursors. *Nature.* 444:203–207. doi:10.1038/nature05161

Mangan, P.R., L.E. Harrington, D.B. O'Quinn, W.S. Helms, D.C. Bullard, C.O. Elson, R.D. Hatton, S.M. Wahl, T.R. Schoeb, and C.T. Weaver. 2006. Transforming growth factor-beta induces development of the T(H)17 lineage. *Nature.* 441:231–234. doi:10.1038/nature04754

Martino, G., and S. Pluchino. 2006. The therapeutic potential of neural stem cells. *Nat. Rev. Neurosci.* 7:395–406. doi:10.1038/nrn1908

Moalem, G., R. Leibowitz-Amit, E. Yoles, F. Mor, I.R. Cohen, and M. Schwartz. 1999. Autoimmune T cells protect neurons from secondary degeneration after central nervous system axotomy. *Nat. Med.* 5:49–55. doi:10.1038/4734

Molina-Holgado, E., J.M. Vela, A. Arévalo-Martín, and C. Guaza. 2001. LPS/IFN-gamma cytotoxicity in oligodendroglial cells: role of nitric oxide and protection by the anti-inflammatory cytokine IL-10. *Eur. J. Neurosci.* 13:493–502. doi:10.1046/j.0953-816x.2000.01412.x

Monje, M.L., H. Toda, and T.D. Palmer. 2003. Inflammatory blockade restores adult hippocampal neurogenesis. *Science.* 302:1760–1765. doi:10.1126/science.1088417

Moore, K.W., R. de Waal Malefyt, R.L. Coffman, and A. O'Garra. 2001. Interleukin-10 and the interleukin-10 receptor. *Annu. Rev. Immunol.* 19:683–765. doi:10.1146/annurev.immunol.19.1.683

Moshiri, A., J. Close, and T.A. Reh. 2004. Retinal stem cells and regeneration. *Int. J. Dev. Biol.* 48:1003–1014. doi:10.1387/ijdb.041870am

Mosser, D.M., and J.P. Edwards. 2008. Exploring the full spectrum of macrophage activation. *Nat. Rev. Immunol.* 8:958–969. doi:10.1038/nri2448

Movahedi, K., M. Guilliams, J. Van den Bossche, R. Van den Bergh, C. Gysemans, A. Beschin, P. De Baetselier, and J.A. Van Ginderachter. 2008. Identification of discrete tumor-induced myeloid-derived suppressor cell subpopulations with distinct T cell-suppressive activity. *Blood.* 111:4233–4244. doi:10.1182/blood-2007-07-099226

Nadal-Nicolás, F.M., M. Jiménez-López, P. Sobrado-Calvo, L. Nieto-López, I. Cánovas-Martínez, M. Salinas-Navarro, M. Vidal-Sanz, and M. Agudo. 2009. Brn3a as a marker of retinal ganglion cells: qualitative and quantitative time course studies in naive and optic nerve-injured retinas. *Invest. Ophthalmol. Vis. Sci.* 50:3860–3868. doi:10.1167/iovs.08-3267

Nahrendorf, M., F.K. Swirski, E. Aikawa, L. Stangenberg, T. Wurdinger, J.L. Figueiredo, P. Libby, R. Weissleder, and M.J. Pittet. 2007. The healing myocardium sequentially mobilizes two monocyte subsets with divergent and complementary functions. *J. Exp. Med.* 204:3037–3047. doi:10.1084/jem.20070885

Nickerson, P.E., J.G. Emsley, T. Myers, and D.B. Clarke. 2007. Proliferation and expression of progenitor and mature retinal phenotypes in the adult mammalian ciliary body after retinal ganglion cell injury. *Invest. Ophthalmol. Vis. Sci.* 48:5266–5275. doi:10.1167/iovs.07-0167

Nimmerjahn, A., F. Kirchhoff, and F. Helmchen. 2005. Resting microglial cells are highly dynamic surveillants of brain parenchyma in vivo. *Science.* 308:1314–1318. doi:10.1126/science.1110647

Ohlsson, M., U. Westerlund, I.A. Langmoen, and M. Svensson. 2004. Methylprednisolone treatment does not influence axonal regeneration or degeneration following optic nerve injury in the adult rat. *J. Neuroophthalmol.* 24:11–18.

Pease, M.E., D.J. Zack, C. Berlinicke, K. Bloom, F. Cone, Y. Wang, R.L. Klein, W.W. Hauswirth, and H.A. Quigley. 2009. Effect of CNTF on retinal ganglion cell survival in experimental glaucoma. *Invest. Ophthalmol. Vis. Sci.* 50:2194–2200. doi:10.1167/iovs.08-3013

Pluchino, S., L. Muzio, J. Imitola, M. Deleidi, C. Alfaro-Cervello, G. Salani, C. Porcheri, E. Brambilla, F. Cavasinni, A. Bergamaschi, et al. 2008. Persistent inflammation alters the function of the endogenous brain stem cell compartment. *Brain.* 131:2564–2578. doi:10.1093/brain/awn198

Reh, T.A., and A.J. Fischer. 2006. Retinal stem cells. *Methods Enzymol.* 419:52–73. doi:10.1016/S0076-6879(06)19003-5

Rolls, A., R. Shechter, A. London, Y. Ziv, A. Ronen, R. Levy, and M. Schwartz. 2007. Toll-like receptors modulate adult hippocampal neurogenesis. *Nat. Cell Biol.* 9:1081–1088. doi:10.1038/ncb1629

Rolls, A., R. Shechter, A. London, Y. Segev, J. Jacob-Hirsch, N. Amariglio, G. Rechavi, and M. Schwartz. 2008. Two faces of chondroitin sulfate proteoglycan in spinal cord repair: a role in microglia/macrophage activation. *PLoS Med.* 5:e171. doi:10.1371/journal.pmed.0050171

Schori, H., J. Kipnis, E. Yoles, E. WoldeMussie, G. Ruiz, L.A. Wheeler, and M. Schwartz. 2001. Vaccination for protection of retinal ganglion cells against death from glutamate cytotoxicity and ocular hypertension: implications for glaucoma. *Proc. Natl. Acad. Sci. USA.* 98:3398–3403. doi:10.1073/pnas.041609498

Schori, H., E. Yoles, L.A. Wheeler, T. Raveh, A. Kimchi, and M. Schwartz. 2002. Immune-related mechanisms participating in resistance and susceptibility to glutamate toxicity. *Eur. J. Neurosci.* 16:557–564. doi:10.1046/j.1460-9568.2002.02134.x

Schwartz, M. 2004. Vaccination for glaucoma: dream or reality? *Brain Res. Bull.* 62:481–484. doi:10.1016/S0361-9230(03)00073-X

Schwartz, M., and J. Kipnis. 2007. Model of acute injury to study neuroprotection. *Methods Mol. Biol.* 399:41–53. doi:10.1007/978-1-59745-504-6_4

Shaw, P.J., and P.G. Ince. 1997. Glutamate, excitotoxicity and amyotrophic lateral sclerosis. *J. Neurol.* 244:S3–S14. doi:10.1007/BF03160574

Shechter, R., Y. Ziv, and M. Schwartz. 2007. New GABAergic interneurons supported by myelin-specific T cells are formed in intact adult spinal cord. *Stem Cells.* 25:2277–2282. doi:10.1634/stemcells.2006-0705

Shechter, R., A. Ronen, A. Rolls, A. London, S. Bakalash, M.J. Young, and M. Schwartz. 2008. Toll-like receptor 4 restricts retinal progenitor cell proliferation. *J. Cell Biol.* 183:393–400. doi:10.1083/jcb.200804010

Shechter, R., A. London, C. Varol, C. Raposo, M. Cusimano, G. Yovel, A. Rolls, M. Mack, S. Pluchino, G. Martino, et al. 2009. Infiltrating

blood-derived macrophages are vital cells playing an anti-inflammatory role in recovery from spinal cord injury in mice. *PLoS Med.* 6:e1000113. doi:10.1371/journal.pmed.1000113

Solberg, Y., G. Dubinski, M. Tchirkov, M. Belkin, and M. Rosner. 1999. Methylprednisolone therapy for retinal laser injury. *Surv. Ophthalmol.* 44:S85–S92. doi:10.1016/S0039-6257(99)00093-4

Stanke, J.J., and A.J. Fischer. 2010. Embryonic retinal cells and support to mature retinal neurons. *Invest. Ophthalmol. Vis. Sci.* 51:2208–2218. doi:10.1167/iovs.09-4447

Streilein, J.W. 2003. Ocular immune privilege: therapeutic opportunities from an experiment of nature. *Nat. Rev. Immunol.* 3:879–889. doi:10.1038/nri1224

Tropepe, V., B.L. Coles, B.J. Chiasson, D.J. Horsford, A.J. Elia, R.R. McInnes, and D. van der Kooy. 2000. Retinal stem cells in the adult mammalian eye. *Science.* 287:2032–2036. doi:10.1126/science.287.5460.2032

Vallières, L., I.L. Campbell, F.H. Gage, and P.E. Sawchenko. 2002. Reduced hippocampal neurogenesis in adult transgenic mice with chronic astrocytic production of interleukin-6. *J. Neurosci.* 22:486–492.

Varol, C., L. Landsman, D.K. Fogg, L. Greenshtein, B. Gildor, R. Margalit, V. Kalchenko, F. Geissmann, and S. Jung. 2007. Monocytes give rise to mucosal, but not splenic, conventional dendritic cells. *J. Exp. Med.* 204:171–180. doi:10.1084/jem.20061011

Veldhoen, M., R.J. Hocking, C.J. Atkins, R.M. Locksley, and B. Stockinger. 2006. TGFbeta in the context of an inflammatory cytokine milieu supports de novo differentiation of IL-17-producing T cells. *Immunity.* 24:179–189. doi:10.1016/j.immuni.2006.01.001

Vorwerk, C.K., M.S. Gorla, and E.B. Dreyer. 1999. An experimental basis for implicating excitotoxicity in glaucomatous optic neuropathy. *Surv. Ophthalmol.* 43:S142–S150. doi:10.1016/S0039-6257(99)00017-X

Weber, M.S., T. Prod'homme, S. Youssef, S.E. Dunn, C.D. Rundle, L. Lee, J.C. Patarroyo, O. Stüve, R.A. Sobel, L. Steinman, and S.S. Zamvil. 2007. Type II monocytes modulate T cell-mediated central nervous system autoimmune disease. *Nat. Med.* 13:935–943. doi:10.1038/nm1620

Weinreb, R.N. 2007. Glaucoma neuroprotection: What is it? Why is it needed? *Can. J. Ophthalmol.* 42:396–398. doi:10.3129/i07-045

Werner, S., and R. Grose. 2003. Regulation of wound healing by growth factors and cytokines. *Physiol. Rev.* 83:835–870.

Wohl, S.G., C.W. Schmeer, A. Kretz, O.W. Witte, and S. Isenmann. 2009. Optic nerve lesion increases cell proliferation and nestin expression in the adult mouse eye in vivo. *Exp. Neurol.* 219:175–186. doi:10.1016/j.expneurol.2009.05.008

Wolf, S.A., B. Steiner, A. Wengner, M. Lipp, T. Kammertoens, and G. Kempermann. 2009. Adaptive peripheral immune response increases proliferation of neural precursor cells in the adult hippocampus. *FASEB J.* 23:3121–3128. doi:10.1096/fj.08-113944

Yin, Y., M.T. Henzl, B. Lorber, T. Nakazawa, T.T. Thomas, F. Jiang, R. Langer, and L.I. Benowitz. 2006. Oncomodulin is a macrophage-derived signal for axon regeneration in retinal ganglion cells. *Nat. Neurosci.* 9:843–852. doi:10.1038/nn1701

Yoles, E., and M. Schwartz. 1998. Elevation of intraocular glutamate levels in rats with partial lesion of the optic nerve. *Arch. Ophthalmol.* 116:906–910.

Zhao, X., A.V. Das, F. Soto-Leon, and I. Ahmad. 2005. Growth factor-responsive progenitors in the postnatal mammalian retina. *Dev. Dyn.* 232:349–358. doi:10.1002/dvdy.20290

Ziv, Y., and M. Schwartz. 2008. Orchestrating brain-cell renewal: the role of immune cells in adult neurogenesis in health and disease. *Trends Mol. Med.* 14:471–478. doi:10.1016/j.molmed.2008.09.004

Ziv, Y., N. Ron, O. Butovsky, G. Landa, E. Sudai, N. Greenberg, H. Cohen, J. Kipnis, and M. Schwartz. 2006. Immune cells contribute to the maintenance of neurogenesis and spatial learning abilities in adulthood. *Nat. Neurosci.* 9:268–275. doi:10.1038/nn1629